# 2 SINUSOIDAL-INPUT DESCRIBING FUNCTION (DF)

## 2.0 INTRODUCTION

Of the various describing functions discussed throughout this text, the *sinusoidal-input describing function* is by far the most widely known and used. In the following discussion the abbreviation DF is reserved for reference to this describing function.

As the name implies, the DF is a linearization of a nonlinear element subjected to a sinusoidal input. In the next two chapters we see that different interpretations regarding the origin of this sinusoidal input allow the study of totally unrelated modes of behavior occurring in nonlinear systems. However, in each such study the representation for the nonlinearity is its DF.

According to the theory of optimum quasi-linearization developed in the preceding chapter, the describing function for a nonlinearity driven by an input consisting of just a single sinusoidal component is given by a

specialization of Eqs. (1.5-36). These expressions are repeated here for convenient reference.

$$N_A = n_p + jn_q \tag{2.0-1a}$$

$$n_p = \frac{2}{A}\overline{y(0)\sin\theta} \tag{2.0-1b}$$

$$n_q = \frac{2}{A}\overline{y(0)\cos\theta} \tag{2.0-1c}$$

The nonlinearity input is in this case

$$x(t) = A\sin(\omega t + \theta) \tag{2.0-2}$$

where the amplitude and frequency, $A$ and $\omega$, are deterministic quantities, and $\theta$ is the random phase angle which is uniformly distributed over $2\pi$ radians.

$y(0)$ in Eqs. (2.0-1) is the output of the nonlinearity at an arbitrary time called zero. The output of a nonlinearity is a function of its input, and in some instances the relation is quite complex. To emphasize the fact that $y(t)$ depends on $x(t)$ in some way, we shall indicate in the notation a dependence on the current value of $x(t)$ and its first derivative.

$$y(t) = y[x(t),\dot{x}(t)] \tag{2.0-3}$$

This is not a restriction on the form of the nonlinearity, however. Any functional relation is acceptable. It is required only that the steady-state output history corresponding to a sinusoidal input be defined. In view of Eqs. (2.0-2) and (2.0-3),

$$y(0) = y(A\sin\theta, A\omega\cos\theta) \tag{2.0 4}$$

In general, the expectations indicated in Eqs. (2.0-1) are over all random parameters required to define $y(0)$. For the single-sinusoidal-input case, the only random parameter in the problem is the phase angle $\theta$. The expectation is then a single integral over the range of $\theta$, which can be taken as 0, $2\pi$. The probability density function for this uniformly distributed variable is $1/2\pi$ in that interval. Equations (2.0-1) are thus specialized in this case to

$$n_p = \frac{1}{\pi A}\int_0^{2\pi} y(A\sin\theta, A\omega\cos\theta)\sin\theta\, d\theta \tag{2.0-5a}$$

$$n_q = \frac{1}{\pi A}\int_0^{2\pi} y(A\sin\theta, A\omega\cos\theta)\cos\theta\, d\theta \tag{2.0-5b}$$

Historically, the basis for the DF was established by Krylov's and Bogoliubov's continuation in the field of nonlinear mechanics of an earlier work by Van der Pol. We shall briefly develop and study this basis to see

how it relates to the DF of current usage, derived from a quite different point of view. Once having established the significant relationships involved, the remainder of this chapter is then devoted to DF calculations for a variety of nonlinear elements. Static and dynamic, memoryless and with memory, implicit and explicit nonlinearities are treated. A compilation of the DFs for all the nonlinearities treated, as well as many others, is presented in Appendix B.

## 2.1 ASYMPTOTIC METHODS FOR THE STUDY OF NONLINEAR OSCILLATIONS

Starting with the well-known and extensively developed theory of linear systems, particularly of linear oscillators, a first step in the exploration of nonlinear oscillatory behavior is to study periodic regimes of the system characterized by

$$\ddot{x} + \omega_0^2 x + \mu f(x,\dot{x}) = 0 \tag{2.1-1}$$

where $\mu$ is a small parameter. In the limit as $\mu \to 0$ this system reduces to the classical *linear* oscillator.

By *asymptotic* methods we shall mean *approximating* schemes for the solution of Eq. (2.1-1), which also result in the *exact* solution in the limit as $\mu \to 0$. A great variety of such methods have been developed. Our ultimate objective is to develop methods which are also valid in the limit of large $\mu$, as in the case of discontinuous nonlinearities. Nevertheless, the most intuitive point of view is born in the study of only slightly nonlinear systems.

Since the intent of this section is primarily to place in perspective the DF approach to be thoroughly studied in this and the following two chapters, we discuss only two different asymptotic methods. The two approaches are conventionally called the *perturbation method* and the *method of slowly varying amplitude and phase.*

### PERTURBATION METHOD

Another name by which the general technique is known is the *method of small parameters.* This method was formulated by Poisson (ca. 1830) and studied throughout the nineteenth century by a number of astronomers, including Gylden and Lindstedt, culminating finally in the extensive work of Poincaré. Although the discussion following is without proof of convergence of the solution, a rigorous mathematical justification due to Poincaré (Ref. 42) is available in Stoker (Ref. 49).

For the system of Eq. (2.1-1) assume a solution of the form

$$x(t) = x_0(t) + \mu x_1(t) + \mu^2 x_2(t) + \cdots$$
$$= \sum_{i=0}^{\infty} \mu^i x_i(t) \tag{2.1-2}$$

where $\mu$ is the small parameter to which the nonlinear term is proportional. Substituting $x(t)$ from Eq. (2.1-2) into (2.1-1) gives

$$\sum_{i=0}^{\infty} \mu^i \ddot{x}_i(t) + \omega_0^2 \sum_{i=0}^{\infty} \mu^i x_i(t) = -\mu f\left[\sum_{i=0}^{\infty} \mu^i x_i(t), \sum_{i=0}^{\infty} \mu^i \dot{x}_i(t)\right] \tag{2.1-3}$$

Consider the right-hand member of Eq. (2.1-3) as expanded in a Taylor series about $x(t) = x_0(t)$. This, of course, requires that $f(x,\dot{x})$ be an analytic function. We now argue that, for $\mu \to 0$, the leading term $x_0(t)$ in Eq. (2.1-2) must approach the corresponding exact solution $x(t)$ and that the terms involving $x_i(t)$ for $i \geq 1$ must be of increasingly smaller importance. Thus the initial conditions are distributed according to

$$x_0(0) = x(0) \qquad \dot{x}_0(0) = \dot{x}(0) \tag{2.1-4a}$$

and

$$x_i(0) = 0 \qquad \dot{x}_i(0) = 0 \qquad \text{for } i \geq 1 \tag{2.1-4b}$$

and Eq. (2.1-3) is solved *recursively*, starting with low-ordered $\mu$. Collating terms of like coefficient, $\mu^i$, gives

$$\begin{aligned}
&\mu^0: \quad \ddot{x}_0 + \omega_0^2 x_0 = 0 \\
&\mu^1: \quad \ddot{x}_1 + \omega_0^2 x_1 = -f(x_0,\dot{x}_0) \\
&\mu^2: \quad \ddot{x}_2 + \omega_0^2 x_2 = -\frac{\partial f}{\partial x}(x_0,\dot{x}_0)x_1 - \frac{\partial f}{\partial \dot{x}}(x_0,\dot{x}_0)\dot{x}_1 \\
&\cdots\cdots\cdots\cdots\cdots\cdots\cdots\cdots
\end{aligned} \tag{2.1-5}$$

In this manner the postulated series expansion of $x(t)$ is determined.

A difficulty arises in the solution of this set of equations which, in one form or another, baffled the earlier nineteenth-century astronomers. This is due to the appearance in the solutions they obtained of apparently unbounded functions, called *secular terms*. It is easy to appreciate this difficulty by noting that the first few terms in the series expansion of a perfectly well-behaved bounded function can convey the picture of unboundedness. For example,

$$\sin(\omega_0 + \mu)t = \sin \omega_0 t + \mu t \cos \omega_0 t - \mu^2 \frac{t^2}{2} \sin \omega_0 t + \cdots \tag{2.1-6}$$

Many attempts to remove secular terms were made. One simple approach was to assume a dependence of solution frequency upon solution amplitude, should the physical picture support this observation, by taking

$$\omega^2 = \omega_0^2 + \mu \Psi_1(A) + \mu^2 \Psi_2(A) + \cdots \tag{2.1-7}$$

where $\omega$ is the actual fundamental frequency of the oscillation, and so choosing $\Psi_1(A), \Psi_2(A), \ldots$ as to remove the secular terms as they arise (Ref. 6). Inserting both the expression for $\omega_0^2$ from Eq. (2.1-7) and the series for $x(t)$ from Eq. (2.1-2) into Eq. (2.1-1) and once again collating terms of like coefficient $\mu^i$ give the recursive set of equations

$$\begin{aligned}
\mu^0: &\quad \ddot{x}_0 + \omega^2 x_0 = 0 \\
\mu^1: &\quad \ddot{x}_1 + \omega^2 x_1 = x_0 \Psi_1(A) - f(x_0, \dot{x}_0) \\
\mu^2: &\quad \ddot{x}_2 + \omega^2 x_2 = x_0 \Psi_2(A) + x_1 \Psi_1(A) - \frac{\partial f}{\partial x}(x_0, \dot{x}_0) x_1 - \frac{\partial f}{\partial \dot{x}}(x_0, \dot{x}_0) \dot{x}_1 \\
&\quad \cdots\cdots\cdots\cdots\cdots\cdots\cdots\cdots\cdots\cdots
\end{aligned} \tag{2.1-8}$$

One advantage of the perturbation method is that successive approximations of higher order can be formed in a systematic manner. It is quite useful for the study of both nonoscillatory and oscillatory systems. For the first type, though, a disadvantage is the requirement of an analytic functional description of the nonlinearity; and for the latter type an additional disadvantage is that a special mode of solution is required to eliminate occurrence of the secular terms. In what follows we present another procedure designed rather specifically for nonlinear oscillatory systems, which does not entail either of these disadvantages.

## METHOD OF SLOWLY VARYING AMPLITUDE AND PHASE

For small $\mu$, it is argued, the solution of Eq. (2.1-1) is fundamentally oscillatory in nature. Recognizing this behavior, Van der Pol (1924) proposed a solution of the form

$$x(t) = a(t) \sin \omega_0 t + b(t) \cos \omega_0 t \tag{2.1-9}$$

where $a(t)$ and $b(t)$ are to be determined by the method of *variation of parameters*. The principal feature in this solution is use of the *method of averaging* to reduce the resulting variational equations to autonomous form. Krylov and Bogoliubov (1937) and Bogoliubov and Mitropolsky (1958) follow the same original argument, but use a solution of the form

$$x(t) = A(t) \sin [\omega_0 t + \theta(t)] \tag{2.1-10}$$

As this formulation is fully equivalent, albeit more convenient to work with, than Van der Pol's, we develop the method of slowly varying amplitude and phase after Krylov and Bogoliubov (Ref. 29).

Let us assume the functional time dependence of $A$ and $\theta$ without explicitly indicating it by an appended argument in $t$, and for convenience introduce the parameter $\psi$, defined by

$$\psi = \omega_0 t + \theta \tag{2.1-11}$$

We seek a solution of the form

$$x = A \sin \psi \tag{2.1-12a}$$

$$\dot{x} = A\omega_0 \cos \psi \tag{2.1-12b}$$

which requires the constraint

$$\dot{A} \sin \psi + A\dot{\theta} \cos \psi = 0 \tag{2.1-13}$$

determined by differentiation of Eq. (2.1-10) and comparison of the result with Eq. (2.1-12*b*). Forming the second derivative $\ddot{x}$ by differentiating $\dot{x}$ in Eq. (2.1-12*b*) gives

$$\ddot{x} = \dot{A}\omega_0 \cos \psi - A\omega_0(\omega_0 + \dot{\theta}) \sin \psi \tag{2.1-14}$$

Substituting for $x$ and $\ddot{x}$ in Eq. (2.1-1) and repeating Eq. (2.1-13) gives the variational set

$$\dot{A}\omega_0 \cos \psi - A\omega_0\dot{\theta} \sin \psi = -\mu f(A \sin \psi, A\omega_0 \cos \psi) \tag{2.1-15a}$$

$$\dot{A} \sin \psi + A\dot{\theta} \cos \psi = 0 \tag{2.1-15b}$$

Solving Eqs. (2.1-15) for $\dot{A}$ and $\dot{\theta}$ yields

$$\dot{A} = -\frac{1}{\omega_0} \mu f(A \sin \psi, A\omega_0 \cos \psi) \cos \psi \tag{2.1-16a}$$

$$\dot{\theta} = \frac{1}{A\omega_0} \mu f(A \sin \psi, A\omega_0 \cos \psi) \sin \psi \tag{2.1-16b}$$

At this point we are at an apparent impasse, since this nonautonomous set usually cannot be solved exactly. From the requirement that $\mu$ be small, however, it may be inferred that in general $\dot{A}$ and $\dot{\theta}$ are small, and hence that $A$ and $\theta$ are slowly varying functions of time. We are thus led to consider approximate solutions $\underline{A}$ and $\underline{\theta}$ obtained by an *averaging* of $\dot{A}$ and $\dot{\theta}$ over one complete cycle of the oscillatory solution. Equations (2.1-16) are thereby replaced by the averaged set

$$\dot{A} \approx -\frac{1}{2\pi\omega_0} \int_0^{2\pi} \mu f(A \sin \psi, A\omega_0 \cos \psi) \cos \psi \, d\psi \tag{2.1-17a}$$

$$\dot{\theta} \approx \frac{1}{2\pi\omega_0} \int_0^{2\pi} \frac{1}{A} \mu f(A \sin \psi, A\omega_0 \cos \psi) \sin \psi \, d\psi \tag{2.1-17b}$$

In effecting each of these integrals, $A$ is held constant. Integrating the right-hand member of Eq. (2.1-17*a*) yields a first-order differential equation of the *separable-variables* type in $A$ and $t$. Call the solution of this equation $\underline{A}(t)$. Then, integrating the right-hand member of Eq. (2.1-17*b*), in which $A$ is first brought out from under the integral sign, yields another first-order differential equation. Replacing $A$ by $\underline{A}$, one solves this differential equation

to obtain $\theta(t)$. The first-approximation solution to Eq. (2.1-1) then takes the form of Eq. (2.1-10); i.e., it is $x(t) = \underline{A}(t) \sin [\omega_0 t + \underline{\theta}(t)]$.

The resulting first-order solution, so obtained by Krylov and Bogoliubov (*op. cit.*), is simpler in form than is the solution obtained by the perturbation method. However, higher-order approximations do not follow as simply. Methods of obtaining higher-order approximations are deferred to Chap. 3. It is to be noted that $f(x,\dot{x})$ need not be analytically expressed before computation of the integrals in Eqs. (2.1-17) can be effected. Both discontinuous and continuous nonlinear functions $f(x,\dot{x})$ can be treated with equal ease.

## 2.2 EQUIVALENT LINEARIZATION AND THE DF

Having just studied the method of slowly varying amplitude and phase, we are in a position to interpret the solution obtained in terms of an equivalent linear representation for the nonlinearity $\mu f(x,\dot{x})$. For continuity with what shall become the central part of this and the two following chapters, we rename the nonlinear element

$$y(x,\dot{x}) = \mu f(x,\dot{x}) \tag{2.2-1}$$

and proceed to the concept of harmonic linearization.

### AN INTERPRETATION OF PREVIOUS RESULTS

According to Krylov and Bogoliubov, the solution to

$$\ddot{x} + \omega_0^2 x + y(x,\dot{x}) = 0 \tag{2.2-2}$$

can be sought in the form

$$x = A \sin \psi \tag{2.2-3}$$

where, as shown in the previous section,

$$\begin{aligned} \dot{A} &\approx -\frac{1}{2\pi\omega_0} \int_0^{2\pi} y(A \sin \psi, A\omega_0 \cos \psi) \cos \psi \, d\psi \\ \dot{\theta} &\approx \frac{1}{2\pi A\omega_0} \int_0^{2\pi} y(A \sin \psi, A\omega_0 \cos \psi) \sin \psi \, d\psi \end{aligned} \tag{2.2-4}$$

Let us attempt to identify these results in terms of the solution to an already well-known system, the linear second-order damped oscillator. For this system the differential equation of motion is

$$\ddot{x} + 2\zeta\omega_n \dot{x} + \omega_n^2 x = 0 \tag{2.2-5}$$

where $\zeta$ is the damping ratio, and $\omega_n$ is the natural frequency. The exact solution of this equation can be written in the form

$$\begin{aligned} x &= A_1 e^{-\zeta\omega_n t} \sin\left(\omega_n\sqrt{1-\zeta^2}\, t + \theta_1\right) \\ &= A \sin\left(\omega t + \theta_1\right) \end{aligned} \tag{2.2-6}$$

where $A_1$ and $\theta_1$ are determined by the initial conditions. In any event, the solution is a sinusoid with *amplitude* $A$, where

$$A = A_1 e^{-\zeta\omega_n t} \tag{2.2-7}$$

from which we immediately determine the relationship

$$\frac{\dot{A}}{A} = -\zeta\omega_n \tag{2.2-8}$$

The frequency of the exact solution, squared, is

$$\omega^2 = \omega_n{}^2(1-\zeta^2) \tag{2.2-9}$$

Using the interpretations for $\zeta\omega_n$ and $\omega_n{}^2$ afforded by the above, we may rewrite (2.2-5) in the form

$$\ddot{x} - 2\frac{\dot{A}}{A}\dot{x} + \left[\omega^2 + \left(\frac{\dot{A}}{A}\right)^2\right]x = 0 \tag{2.2-10}$$

Note that, as yet, there is no approximation incorporated in this equation.

The gap in this argument can now be closed, since here we observe that, in accord with the results of Krylov and Bogoliubov [Eqs. (2.2-2) to (2.2-4)], the coefficients of Eq. (2.2-10) can be expressed in the form

$$\ddot{x} + \frac{n_q(A,\omega_0)}{\omega_0}\dot{x} + [\omega_0{}^2 + n_p(A,\omega_0)]x \approx 0 \qquad \omega = \omega_0 + \dot{\theta} \tag{2.2-11}$$

where the following definitions have been made:

$$n_p(A,\omega_0) = \frac{1}{\pi A}\int_0^{2\pi} y(A\sin\psi,\, A\omega_0\cos\psi)\sin\psi\, d\psi \tag{2.2-12a}$$

$$n_q(A,\omega_0) = \frac{1}{\pi A}\int_0^{2\pi} y(A\sin\psi,\, A\omega_0\cos\psi)\cos\psi\, d\psi \tag{2.2-12b}$$

and only terms up to first order in the implicit small parameter $\mu$ have been retained, viz.,

$$\left(\frac{\dot{A}}{A}\right)^2 \approx \left(\frac{\dot{\theta}}{\omega_0}\right)^2 \approx 0 \tag{2.2-13}$$

Comparing Eqs. (2.2-2) and (2.2-11), and calling $s = d/dt$, it is apparent that the linearized version of the original nonlinear term $y(x,\dot{x})$, valid to second

order in the implicit small parameter, is

$$y(x,\dot{x}) \approx \left[ n_p(A,\omega_0) + \frac{n_q(A,\omega_0)}{\omega_0} s \right] x \tag{2.2-14}$$

*The above linearization is fundamental to all that follows, and was, in fact, the first derivation of the DF.* What has, in effect, been done is the replacement of a small nonlinearity by a linear *proportional plus derivative* network, whose coefficients are *not* constant, but rather are functions of the *amplitude* and *frequency* of the system oscillation. This procedure is called *harmonic linearization*, particularly in the Russian literature.

It is significant to note here the suggestion by Krylov and Bogoliubov that this linearization (derived in terms of a second-order system) also be used for nonlinearities in systems of higher order than second. It should also be noted that this linearization is exactly that which results from the general theory of Chap. 1. In particular, Eqs. (2.2-12) are identical with Eqs. (2.0-5).

## PHYSICALLY MOTIVATED DF DEFINITION

During the years 1947 to 1950, in at least five different countries a new point of view came into being. This new point of view was essentially a physically motivated harmonic linearization, which, as we shall see, yields results equivalent to those derived by Krylov and Bogoliubov. Kochenburger (Ref. 27) is generally credited with its introduction in the United States, while Tustin (Ref. 52) of England, Oppelt (Ref. 41) of Germany, Goldfarb (Ref. 15) of Russia, and Dutilh (Ref. 10) of France played similar roles in their respective countries. Since the time of appearance of the papers cited above, a veritable wealth of material has been published relating to the DF and modifications thereof.

It is DF philosophy simply to replace a system nonlinearity by a linear gain, chosen in a fashion which renders similar the responses of the nonlinearity and its approximation, in some sense, to the same sinusoidal input. This is an attempt to extend the transfer function concept of linear-system studies to the nonlinear-system problem. In this vein we observe that, if a nonlinearity $y(x,\dot{x})$ is excited by a sinusoidal input ($\psi = \omega t$),

$$x = A \sin \psi \tag{2.2-15}$$

then the output is expressible by the Fourier series expansion[1]

$$y(A \sin \psi, A\omega \cos \psi) = \sum_{n=1}^{\infty} A_n(A,\omega) \sin [n\omega t + \varphi_n(A,\omega)] \tag{2.2-16}$$

[1] No output dc term is present since in this chapter we restrict our attention to odd nonlinearities. Other nonlinearities are treated in Chap. 6.

and the sinusoidal-input describing function (DF), denoted $N(A,\omega)$, is by definition

$$N(A,\omega) = \frac{\text{phasor representation of output component at frequency } \omega}{\text{phasor representation of input component at frequency } \omega}$$

$$= \frac{A_1(A,\omega)}{A} e^{j\varphi_1(A,\omega)} \tag{2.2-17}$$

In other words, *the DF is the complex fundamental-harmonic gain of a nonlinearity in the presence of a driving sinusoid.*

The concepts of transfer magnitude and phase changes are embodied in this definition, a direct carry-over from familiar linear theory. In fact, the DF for a nonlinear element is *analogous* to the transfer function for a linear element, reducing *identically* to this transfer function in the purely linear case. We must note, however, that whereas for a linear device the response to an infinite spectrum of sinusoids *completely* defines the response to any other form of excitation, for a nonlinear device the response to an infinite spectrum of sinusoids is *not* definitive about the response to other inputs. *Linear superposition is not valid.* Nevertheless, the DF does lead to simple analysis and synthesis techniques for nonlinear systems which are reminiscent of the familiar frequency response methods exploited so successfully in linear-system analysis and synthesis.

A pictorial view of the DF, including all higher harmonics which are excluded in the DF formulation (collectively called the *residual*), is shown in Fig. 2.2-1.

An equation for the DF in terms of $y(x,\dot{x})$ is easily obtained. Multiplying both sides of Eq. (2.2-16) by either sin $\psi$ or cos $\psi$, and integrating to

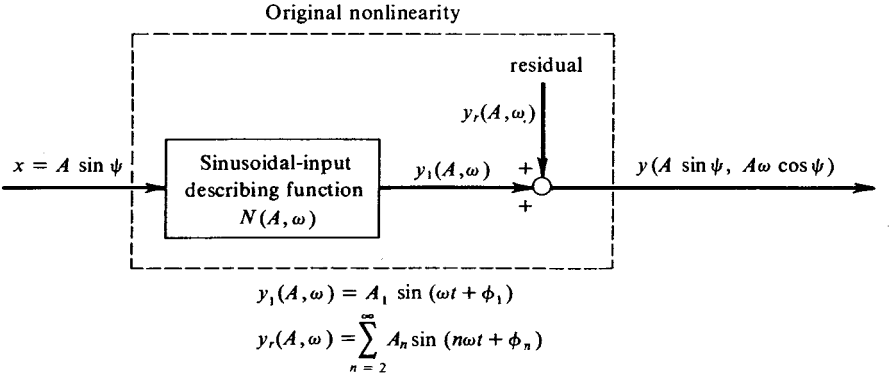


*Figure 2.2-1 Definition of the DF.*

determine the first Fourier coefficients, we find the relationships

$$\begin{aligned} A_1 \cos \varphi_1 &= \frac{1}{\pi} \int_0^{2\pi} y(A \sin \psi, A\omega \cos \psi) \sin \psi \, d\psi \\ A_1 \sin \varphi_1 &= \frac{1}{\pi} \int_0^{2\pi} y(A \sin \psi, A\omega \cos \psi) \cos \psi \, d\psi \end{aligned} \tag{2.2-18}$$

Now, multiplying the second of these equations by $j$, adding the two equations, and dividing both sides of the resultant equation by $A$, we get

$$\frac{A_1}{A} e^{j\varphi_1} = \frac{j}{\pi A} \int_0^{2\pi} y(A \sin \psi, A\omega \cos \psi) e^{-j\psi} \, d\psi \tag{2.2-19}$$

where the relationship

$$e^{j\varphi} = \cos \varphi + j \sin \varphi$$

has been used. Comparing Eqs. (2.2-17) and (2.2-19), the equation for the DF in terms of the system nonlinearity becomes

$$N(A,\omega) = \frac{j}{\pi A} \int_0^{2\pi} y(A \sin \psi, A\omega \cos \psi) e^{-j\psi} \, d\psi \tag{2.2-20}$$

Before attempting to tie in this result with the linearization of Krylov and Bogoliubov, we first observe the relation of this DF to mean-squared approximation error.

### A PROPERTY OF THE DF

Historically, the DF as a linearizing complex gain was defined as opposed to having been derived. It was then noted that the equivalent linearization thus defined also minimized the mean-squared approximation error. This observation results from the following calculation.

Calling the magnitude and phase shift of the linearizing complex gain $\rho_N$ and $\theta_N$, respectively, we seek to minimize the following error measure:

$$\overline{e^2} = \frac{\omega}{2\pi} \int_0^{2\pi/\omega} e^2(t) \, dt \tag{2.2-21}$$

where

$$\begin{aligned} e &= y(x,\dot{x}) - y_{\text{approx}}(A,\omega) \\ &= y(A \sin \psi, A\omega \cos \psi) - A\rho_N \sin (\omega t + \theta_N) \end{aligned} \tag{2.2-22}$$

A stationary point of Eq. (2.2-21) exists when, simultaneously,

$$\frac{\partial \overline{e^2}}{\partial \rho_N} = \frac{\partial \overline{e^2}}{\partial \theta_N} = 0 \tag{2.2-23}$$

Differentiation with respect to $\rho_N$ yields, after simplification,

$$\rho_N = \frac{\omega}{\pi A} \int_0^{2\pi/\omega} y(A \sin \psi, A\omega \cos \psi) \sin (\omega t + \theta_N)\, dt \tag{2.2-24}$$

Similarly, differentiation with respect to $\theta_N$ yields, after simplification,

$$\frac{\omega}{\pi A} \int_0^{2\pi/\omega} y(A \sin \psi, A\omega \cos \psi) \cos (\omega t + \theta_N)\, dt = 0 \tag{2.2-25}$$

Equations (2.2-24) and (2.2-25) can be combined in the form

$$\begin{aligned} \rho_N &= \frac{\omega}{\pi A} \int_0^{2\pi/\omega} y(A \sin \psi, A\omega \cos \psi)[\sin (\omega t + \theta_N) + j \cos (\omega t + \theta_N)]\, dt \\ &= j \frac{\omega}{\pi A} e^{-j\theta_N} \int_0^{2\pi/\omega} y(A \sin \psi, A\omega \cos \psi) e^{-j\omega t}\, dt \end{aligned} \tag{2.2-26}$$

which can in turn be rearranged to yield ($\psi = \omega t$)

$$\rho_N e^{j\theta_N} = \frac{j}{\pi A} \int_0^{2\pi} y(A \sin \psi, A\omega \cos \psi) e^{-j\psi}\, d\psi \tag{2.2-27}$$

By comparison with Eq. (2.2-20) we conclude that the describing function defined as the first harmonic gain of a nonlinearity driven by a sinusoid also minimizes the mean-squared error in the linearizing approximation.

For the general theory of quasi-linear approximation developed in Chap. 1, minimum mean-squared approximation error was taken as the starting point. This defining condition permits the *derivation* of describing functions for nonlinearities driven by any form of input, whereas the first-harmonic-gain concept is applicable only to sinusoidal inputs. It was also shown there that the equivalent complex gain of a nonlinearity to a sinusoid input component in the presence of any other independent input components is the first harmonic gain of a pseudo-nonlinearity, defined by averaging over the effects of the other input components. If the input consists of a sinusoid only, this reduces to the first harmonic gain of the actual nonlinearity.

## SUMMARY OF DF FORMS

The DF has been written both in the form of a dynamic proportional plus derivative element [Eq. (2.2-14)] and in the form of a static complex gain [Eq. (2.2-20)]. These seemingly different linearizations can be at once

reconciled by expanding the right-hand side of Eq. (2.2-20). Expansion yields

$$N(A,\omega) = \frac{j}{\pi A}\int_0^{2\pi} y(A\sin\psi, A\omega\cos\psi)e^{-j\psi}\,d\psi$$

$$= \frac{j}{\pi A}\int_0^{2\pi} y(A\sin\psi, A\omega\cos\psi)(\cos\psi - j\sin\psi)\,d\psi$$

$$= n_p(A,\omega) + jn_q(A,\omega) \tag{2.2-28}$$

where $n_p(A,\omega)$ and $n_q(A,\omega)$, defined earlier in Eqs. (2.2-12) and repeated here for convenience, are

$$n_p(A,\omega) = \frac{1}{\pi A}\int_0^{2\pi} y(A\sin\psi, A\omega\cos\psi)\sin\psi\,d\psi \tag{2.2-29a}$$

$$n_q(A,\omega) = \frac{1}{\pi A}\int_0^{2\pi} y(A\sin\psi, A\omega\cos\psi)\cos\psi\,d\psi \tag{2.2-29b}$$

Observing the complex-gain point of view, it follows from Eq. (2.2-28) that $n_p(A,\omega)$ and $n_q(A,\omega)$ are the *in-phase* and *quadrature* gains of the nonlinearity. That is, $An_p$ is the in-phase (sin) component of the nonlinearity output, and $An_q$ is the *quadrature* (cos) component of the nonlinearity output, referred to the input. Hence the mnemonic use of $p$ and $q$.

Continuing, let us interpret the complex gain $N(A,\omega)$ in Eq. (2.2-28) as a linear operator which, acting upon a sinusoidal input $x = A\sin\omega t$, gives the appropriately phased sinusoidal output. Calling $s = d/dt$, this is equivalent to writing

$$N(A,\omega) = n_p(A,\omega) + \frac{n_q(A,\omega)}{\omega}s \tag{2.2-30}$$

which, of course, is precisely the result of Eq. (2.2-14).

Summarizing the above discussion, we have the following useful DF representations for a nonlinearity:

■ DF as a proportional plus derivative element

$$N(A,\omega) = n_p(A,\omega) + \frac{n_q(A,\omega)}{\omega}s \tag{2.2-31}$$

■ DF as a complex gain

$$N(A,\omega) = n_p(A,\omega) + jn_q(A,\omega) \tag{2.2-32}$$

or

$$N(A,\omega) = \rho_N(A,\omega)e^{j\theta_N(A,\omega)} \tag{2.2-33}$$

where the magnitude–phase angle representation is found according to

$$\rho_N(A,\omega) = \sqrt{n_p^2(A,\omega) + n_q^2(A,\omega)}$$
$$\theta_N(A,\omega) = \tan^{-1}\frac{n_q(A,\omega)}{n_p(A,\omega)} \tag{2.2-34}$$

the corresponding set of inverse relationships being

$$n_p(A,\omega) = \rho_N(A,\omega)\cos\theta_N(A,\omega)$$
$$n_q(A,\omega) = \rho_N(A,\omega)\sin\theta_N(A,\omega) \tag{2.2-35}$$

Throughout the development thus far we have assumed a nonlinearity output which, in general, is a function of the input as well as its derivative(s). Certain computational simplifications occur when the nonlinearity is static, and additional computational ease results when the static nonlinearity is odd. For example:

■ DF calculation for a general dynamic nonlinearity $[y = y(x,\dot{x})]$

$$N(A,\omega) = \frac{j}{\pi A}\int_0^{2\pi} y(A\sin\psi,\ A\omega\cos\psi)e^{-j\psi}\,d\psi \tag{2.2-36}$$

■ DF calculation for a general static nonlinearity $[y = y(x)]$

$$N(A) = \frac{j}{\pi A}\int_0^{2\pi} y(A\sin\psi)e^{-j\psi}\,d\psi \tag{2.2-37}$$

■ DF calculation for an odd static nonlinearity $[y(x) = -y(-x)]$

$$N(A) = \frac{2j}{\pi A}\int_0^{\pi} y(A\sin\psi)e^{-j\psi}\,d\psi \tag{2.2-38}$$

Single-valued characteristics are termed *memoryless;* multivalued characteristics are said to possess *memory.* For all memoryless nonlinearities, $n_q(A,\omega) = 0$. The ranges of integration can be further restricted. For example:

■ DF calculation for a general memoryless static nonlinearity

$$N(A) = \frac{2}{\pi A}\int_{-\pi/2}^{\pi/2} y(A\sin\psi)\sin\psi\,d\psi \tag{2.2-39}$$

■ DF calculation for an odd memoryless static nonlinearity

$$N(A) = \frac{4}{\pi A}\int_0^{\pi/2} y(A\sin\psi)\sin\psi\,d\psi \tag{2.2-40}$$

The remainder of this chapter is devoted to various aspects of the computation of DFs in the complex-gain representation. The questions of DF usage, DF accuracy, and DF validity are deferred to the following chapter.

## 2.3 DF CALCULATION FOR FREQUENCY-INDEPENDENT NONLINEARITIES

In this section we deal with nonlinearities whose input-output characteristics fall into the class defined by

$$y = y(x)$$

Such nonlinearities are *static*, displaying no dependence upon the input derivatives. At present, it is further required that the nonlinear characteristics possess *odd symmetry*. This requirement is expressed as

$$y(x) = -y(-x)$$

It is to be noted that DF determination for *asymmetric* nonlinearities is straightforward. DF application in such instances, however, is confounded by the presence of a nonlinearity output bias whose presence is not accounted for in the DF formulation. This difficulty may be overcome by artificially shifting the nonlinearity characteristic along its output axis to the point at which an input sinusoid results in an unbiased output. A less artificial approach to this problem is taken in Sec. 6.6, however, in which such nonlinearities are dealt with directly.

### GAIN-CHANGING ELEMENT

The symmetrical gain-changing element with two slope discontinuities is shown in Fig. 2.3-1*a*. One common mechanical system giving rise to such a force-displacement characteristic is the dynamic vibration mount, for which a (massless) spring arrangement is depicted in Fig. 2.3-1*b*. In terms of the spring constants defined in the illustration, it is clear that $m_1 = 2k_1$ and $m_2 = 2(k_1 + k_2)$. For this nonlinearity the actual response to a driving sinusoid and the corresponding first harmonic are shown in Fig. 2.3-2. Since the response is not frequency-dependent, the independent variable of the input and output graphs has been chosen as the angle $\psi$ (where $\psi = \omega t$). There are two regions of interest, those in which $y$ assumes different dependencies upon $x$. Let us define the angle $\psi_1$ according to

$$A \sin \psi_1 = \delta$$

or

$$\psi_1 = \sin^{-1} \frac{\delta}{A} \tag{2.3-1}$$

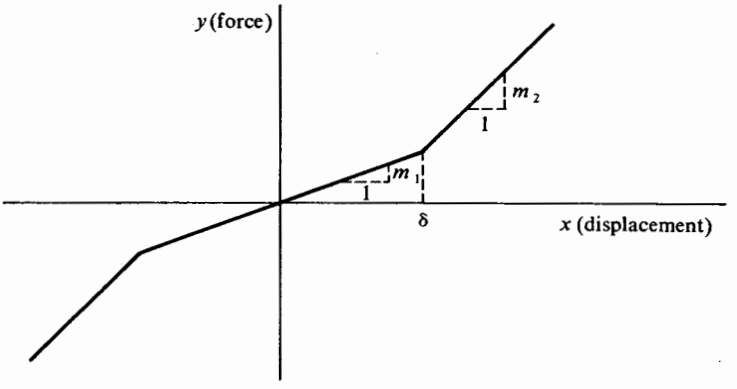


(*a*) Input-output characteristic

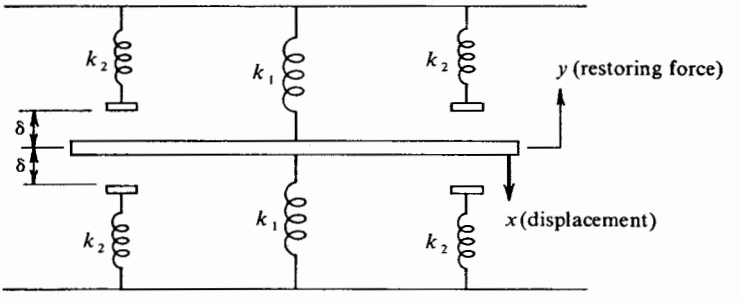


(*b*) Parallel translation spring assembly

***Figure 2.3-1*** *Gain-changing nonlinear element.*

Then the two regions of interest are defined in terms of $\psi_1$ as follows:

$$\begin{aligned} 0 < \psi \leq \psi_1 \qquad & y = m_1 x \\ \psi_1 < \psi \leq \frac{\pi}{2} \qquad & y = (m_1 - m_2)\delta + m_2 x \end{aligned} \tag{2.3-2}$$

We may proceed directly to the calculation of $N(A)$ after Eq. (2.2-40).

$$\begin{aligned} N(A) &= \frac{4}{\pi A}\int_0^{\pi/2} y(A \sin \psi) \sin \psi \, d\psi \\ &= \frac{4}{\pi A}\int_0^{\psi_1} m_1 A \sin^2 \psi \, d\psi + \frac{4}{\pi A}\int_{\psi_1}^{\pi/2} [(m_1 - m_2)\delta + m_2 A \sin \psi] \sin \psi \, d\psi \\ &= \frac{2(m_1 - m_2)}{\pi}\left(\psi_1 - \frac{1}{2}\sin 2\psi_1 + 2\frac{\delta}{A}\cos \psi_1\right) + m_2 \end{aligned} \tag{2.3-3}$$

Equations (2.3-1) and (2.3-3) define the DF for the gain-changing nonlinearity. These may be combined, with the result

$$N(A) = \frac{2(m_1 - m_2)}{\pi}\left[\sin^{-1}\frac{\delta}{A} + \frac{\delta}{A}\sqrt{1 - \left(\frac{\delta}{A}\right)^2}\right] + m_2 \qquad (2.3\text{-}4)$$

Note that this result is valid only for $A \geq \delta$. For $A < \delta$, $N(A) = m_1$, which is the linear gain.

It is worthwhile to observe that in deriving the DF for this gain-changing nonlinearity we have simultaneously accomplished the DF derivation for some simpler nonlinearities. For example, as can be seen from Fig. 2.3-1*a*, setting $m_1 = 0$ results in the dead-zone characteristic; setting $m_2 = 0$ results in the saturation characteristic; setting $m_2 = 0$ and simultaneously $m_1\delta = D$, $m_1 \to \infty$, results in the ideal-relay characteristic; and, of course, setting $m_1 = m_2$ results in the linear-gain characteristic. Figure 2.3-3 illustrates each of the above-mentioned nonlinearities, together with the appropriate DFs as derived from Eq. (2.3-4).

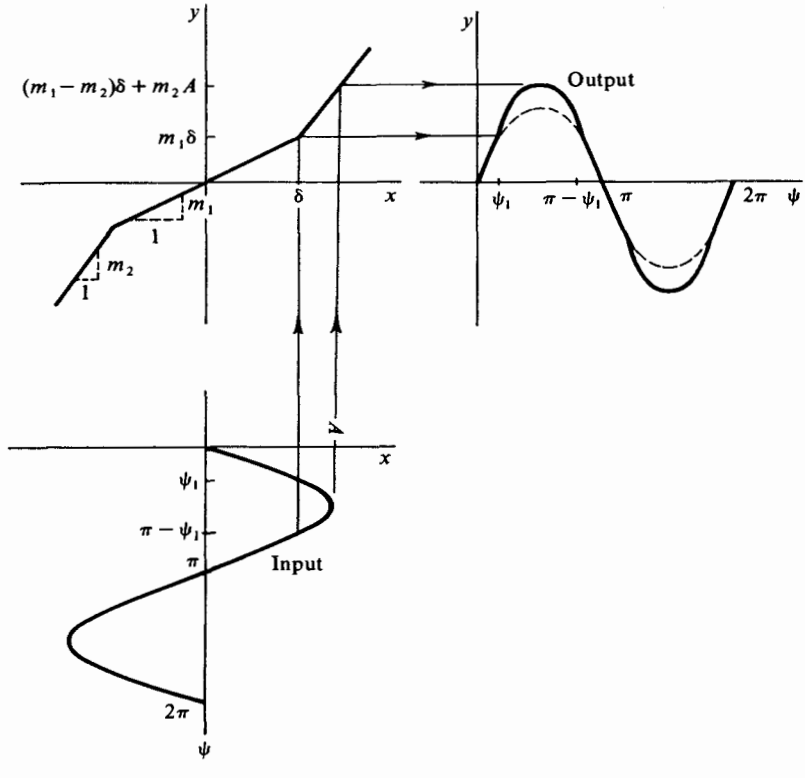


***Figure 2.3-2*** *Input-output relationship for a gain-changing nonlinearity.*

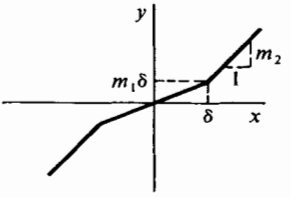


$$N(A) = m_1 \qquad A \le \delta$$

$$= \frac{2(m_1 - m_2)}{\pi}\left[\sin^{-1}\left(\frac{\delta}{A}\right) + \left(\frac{\delta}{A}\right)\sqrt{1 - \left(\frac{\delta}{A}\right)^2}\right] + m_2 \qquad A > \delta$$

(*a*) Gain-changing element

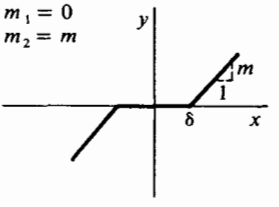


$$N(A) = 0 \qquad A \le \delta$$

$$= \frac{m}{\pi}\left[\pi - 2\sin^{-1}\left(\frac{\delta}{A}\right) - 2\left(\frac{\delta}{A}\right)\sqrt{1 - \left(\frac{\delta}{A}\right)^2}\right] \qquad A > \delta$$

(*b*) Dead zone

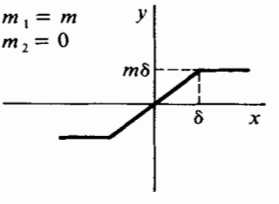


$$N(A) = m \qquad A \le \delta$$

$$= \frac{2m}{\pi}\left[\sin^{-1}\left(\frac{\delta}{A}\right) + \left(\frac{\delta}{A}\right)\sqrt{1 - \left(\frac{\delta}{A}\right)^2}\right] \qquad A > \delta$$

(*c*) Saturation

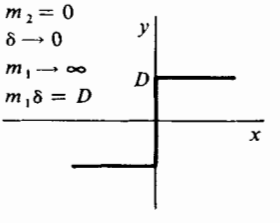


$$N(A) = \frac{4m_1\delta}{\pi A} = \frac{4D}{\pi A}$$

(*d*) Ideal relay

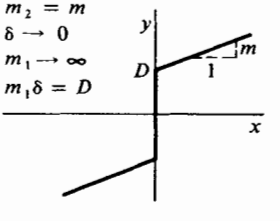


$$N(A) = \frac{4D}{\pi A} + m$$

(*e*) Preload

***Figure 2.3-3*** *DFs for the gain-changing element and related nonlinearities.*

Examination of the DFs for Fig. 2.3-3*a* to *c* reveals that a single functional form is recurrent. For this form we shall coin the name *saturation function* and the designation $f(\delta/A)$, where

$$f\left(\frac{\delta}{A}\right) = \begin{cases} \dfrac{2}{\pi}\left[\sin^{-1}\dfrac{\delta}{A} + \dfrac{\delta}{A}\sqrt{1-\left(\dfrac{\delta}{A}\right)^2}\right] & \text{for } \dfrac{\delta}{A} \leq 1 \\ 1 & \text{for } \dfrac{\delta}{A} > 1 \end{cases} \tag{2.3-5}$$

A plot of $f(\delta/A)$ appears in Fig. 2.3-4. The ordinate scale is linear (rather than logarithmic, which form we shall find quite convenient in actual DF use) in order that the algebraic operations of addition and subtraction may be easily performed during DF calculation. Appendix A is an amplitude-ratio–decibel conversion table with which logarithmic DF representation

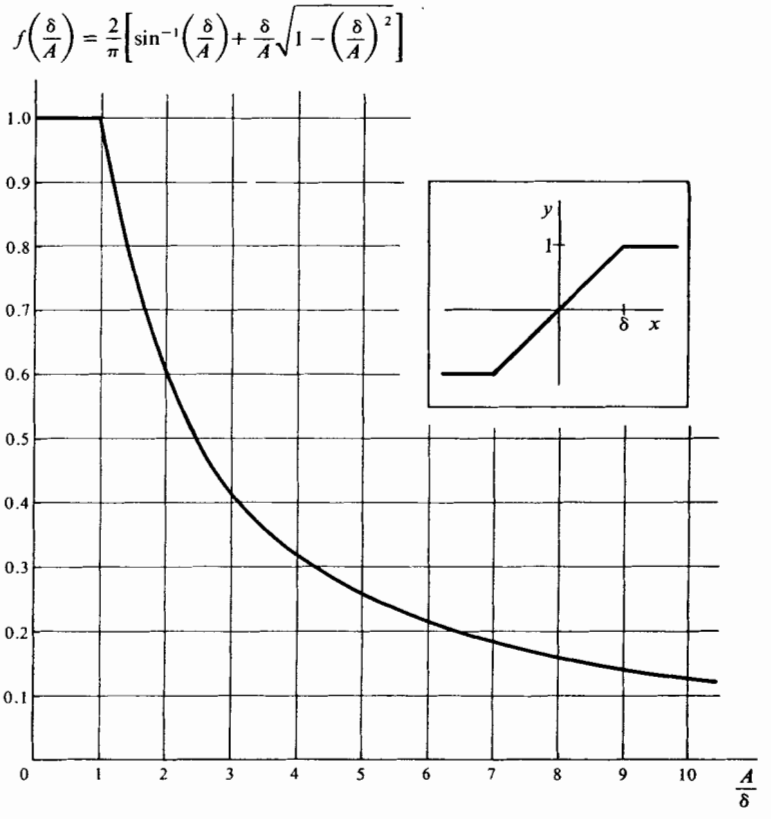


*Figure 2.3-4 Saturation function.*

may be accomplished conveniently, wherever desired. In terms of the saturation function $f(\delta/A)$, we have[1]

Gain-changing element:

$$N(A) = (m_1 - m_2)f\left(\frac{\delta}{A}\right) + m_2 \tag{2.3-6}$$

Dead zone:

$$N(A) = m\left[1 - f\left(\frac{\delta}{A}\right)\right] \tag{2.3-7}$$

Saturation:

$$N(A) = mf\left(\frac{\delta}{A}\right) \tag{2.3-8}$$

Observe that Fig. 2.3-4 is a normalized plot of the saturation DF; hence the name saturation function.

## GENERAL PIECEWISE-LINEAR ODD MEMORYLESS NONLINEARITY

We are now in a position to consider a fairly general case, namely, one where the nonlinear characteristic is any piecewise-linear odd memoryless and frequency-independent function.[2] Figure 2.3-5 illustrates a typical four-segment characteristic (first quadrant only, eight segments in all). All $\delta_i$'s

[1] This form of DF presentation was motivated by the work of Magnus (Ref. 36), who used a slightly less compact notation. See Graham and McRuer (Ref. 16) for details of Magnus' presentation.

[2] A similar development is given by Gille et al. (Ref. 14).

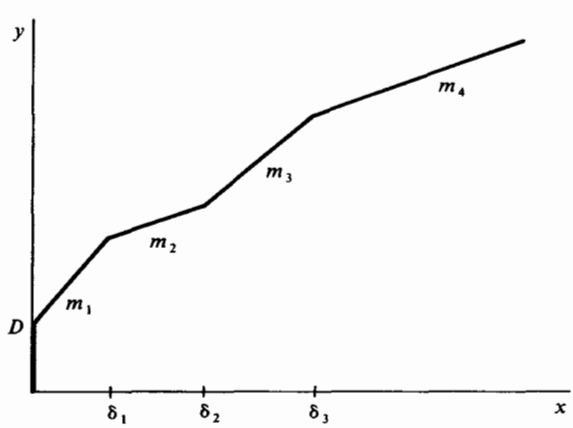


***Figure 2.3-5*** *General piecewise-linear odd memoryless nonlinearity.*

indicate abscissa breakpoints, and $m_i$ indicates the slope occurring in the range $\delta_{i-1} < x \leq \delta_i$. The nonlinearity output $y$ in terms of its input $x$ can be written in the particular form

$$\begin{aligned}
&0 < x \leq \delta_1 \qquad y = m_1 x + D \\
&\delta_1 < x \leq \delta_2 \qquad y = (m_1 - m_2)\delta_1 + m_2 x + D \\
&\delta_2 < x \leq \delta_3 \qquad y = (m_1 - m_2)\delta_1 + (m_2 - m_3)\delta_2 + m_3 x + D \\
&\delta_3 < x \qquad y = (m_1 - m_2)\delta_1 + (m_2 - m_3)\delta_2 + (m_3 - m_4)\delta_3 \\
&\qquad\qquad + m_4 x + D
\end{aligned} \tag{2.3-9}$$

As before, the input is taken as a sinusoid

$$x = A \sin \psi$$

and we may directly compute the DF for various ranges of $A$. In the first range ($0 < A \leq \delta_1$), behavior is like that of a preload nonlinearity. The DF in this range is therefore as given in Fig. 2.3-3*e*. Continuing in other ranges, we note that the DF can very conveniently be described in terms of the saturation function, $f(\delta/A)$. It is readily verified that

$$N(A) = \frac{4D}{\pi A} + (m_1 - m_2) f\left(\frac{\delta_1}{A}\right) + (m_2 - m_3) f\left(\frac{\delta_2}{A}\right) + (m_3 - m_4) f\left(\frac{\delta_3}{A}\right) + m_4 \tag{2.3-10}$$

The reader may show that $N(A)$ is appropriately defined over *all* $A$. Clearly, this sequence can be directly extended by induction to an $n$-segment nonlinearity. Moreover, the actual magnitude of the composite nonlinearity DF can be obtained easily by repeated use of Fig. 2.3-4.

**Example 2.3-1** Derive the DF for the piecewise-linear nonlinearity containing dead zone, a linear band, and saturation (Fig. 2.3-6).

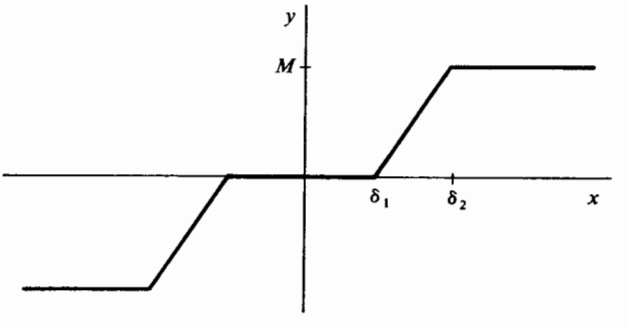


*Figure 2.3-6 Nonlinear characteristic with dead zone, a linear band, and saturation.*

By observing that the more general nonlinearity of Fig. 2.3-5 is reducible to the specific case at hand under the value assignments

$$D = 0, \qquad m_2 = \frac{M}{\delta_2 - \delta_1}, \qquad m_1 = m_3 = m_4 = 0$$

we obtain directly from Eq. (2.3-10)

$$N(A) = \frac{M}{\delta_2 - \delta_1}\left[f\left(\frac{\delta_2}{A}\right) - f\left(\frac{\delta_1}{A}\right)\right] \tag{2.3-11}$$

which takes on the following special values in the ranges indicated:

$$\begin{aligned} 0 < A \leq \delta_1 \qquad & N(A) = 0 \\ \delta_1 < A \leq \delta_2 \qquad & N(A) = \frac{M}{\delta_2 - \delta_1}\left[1 - f\left(\frac{\delta_1}{A}\right)\right] \\ \delta_2 < A \qquad & N(A) = \frac{M}{\delta_2 - \delta_1}\left[f\left(\frac{\delta_2}{A}\right) - f\left(\frac{\delta_1}{A}\right)\right] \end{aligned}$$

## QUANTIZER

A very useful DF in the study of systems containing a linear analog-digital converter is that for the staircase, or quantizer, nonlinearity, shown in Fig. 2.3-7. For all continuous inputs $x$, the output can assume only the discrete values 0, $\pm D$, $\pm 2D$, etc.; hence the name suggesting quantum jumps.

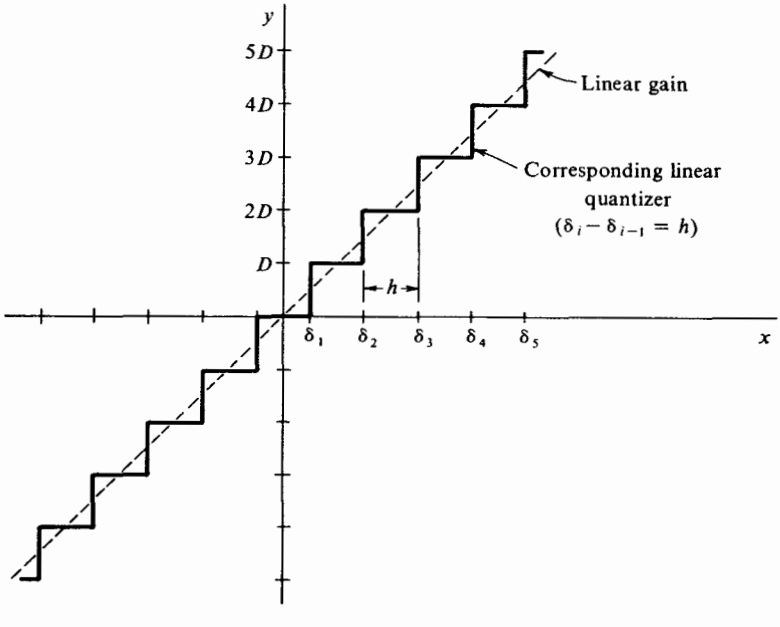


*Figure 2.3-7 Linear quantizer characteristic.*

Call the abscissa breakpoints $\delta_1, \delta_2, \ldots, \delta_n$, in a gesture of generality. Then the DF can be determined as follows (for $A > \delta_n$):

$$\begin{aligned} N(A) &= \frac{4}{\pi A}\int_0^{\pi/2} y(A\sin\psi)\sin\psi\, d\psi \\ &= \frac{4}{\pi A}\left(\int_0^{\psi_1} 0\sin\psi\, d\psi + \int_{\psi_1}^{\psi_2} D\sin\psi\, d\psi + \cdots + \int_{\psi_n}^{\pi/2} nD\sin\psi\, d\psi\right) \\ &= \frac{4D}{\pi A}(\cos\psi_1 + \cos\psi_2 + \cdots + \cos\psi_n) \end{aligned} \tag{2.3-12}$$

where

$$\psi_i = \sin^{-1}\frac{\delta_i}{A} \tag{2.3-13}$$

Hence we determine that the DF is given by

$$\begin{aligned} &0 < A \le \delta_1 && N(A) = 0 \\ &\delta_1 < A \le \delta_2 && N(A) = \frac{4D}{\pi A}\sqrt{1 - \left(\frac{\delta_1}{A}\right)^2} \\ &\delta_2 < A \le \delta_3 && N(A) = \frac{4D}{\pi A}\left[\sqrt{1 - \left(\frac{\delta_1}{A}\right)^2} + \sqrt{1 - \left(\frac{\delta_2}{A}\right)^2}\right] \\ &\cdots\cdots\cdots\cdots\cdots\cdots\cdots\cdots\cdots\cdots\cdots\cdots\cdots\cdots\cdots\cdots \\ &\delta_n < A && N(A) = \frac{4D}{\pi A}\sum_{i=1}^{n}\sqrt{1 - \left(\frac{\delta_i}{A}\right)^2} \end{aligned} \tag{2.3-14}$$

A plot of the DF for the *linear* quantizer, $\delta_i = [(2i - 1)/2]h$, where $h$ is the uniform input breakpoint increment, is shown in Appendix B. Dotted lines indicate the DFs for quantizers of various numbers of output levels. The three-output-level case, for example, corresponds to the relay with dead-zone nonlinearity. With increasing numbers of output levels, the quantizer approaches a linear gain to an increasingly better degree; hence the magnitude of $N(A)$ approaches unity.

## POLYNOMIAL-TYPE NONLINEARITIES

Polynomial functions are particularly useful because of the relative ease with which they may be chosen to closely fit given nonlinear characteristics. The analytic process of curve fitting will not be discussed here, but may be found in a variety of texts.[1] Further, an experimental determination of

[1] See, for example, Ref. 40.

nonlinearity form may be well related to a polynomial fit, either by sinusoidal testing or growing harmonic exponential testing (Ref. 35).

The input-output characteristic for an *odd* $n$th-order polynomial-type nonlinearity is of the form ($n$ is a positive odd integer in this equation)

$$y = c_n x^n + c_{n-1} x^{n-2} |x| + \cdots + c_2 x |x| + c_1 x \tag{2.3-15}$$

The general term of Eq. (2.3-15) can be rewritten as (arbitrary $n$)

$$y = \begin{cases} c_n x^n & x \geq 0 \\ -c_n |x^n| & x < 0 \end{cases} \tag{2.3-16}$$

which is an odd function of $x$. The DF for the general odd polynomial term is therefore computed by integrating over the interval $0 < \psi < \pi/2$, as follows:

$$\begin{aligned} N(A) &= \frac{4}{\pi A} \int_0^{\pi/2} y(A \sin \psi) \sin \psi \, d\psi \\ &= \frac{4}{\pi A} \int_0^{\pi/2} c_n (A \sin \psi)^n \sin \psi \, d\psi \\ &= \frac{4}{\pi} c_n A^{n-1} \int_0^{\pi/2} \sin^{n+1} \psi \, d\psi \\ &= \frac{2c_n}{\sqrt{\pi}} A^{n-1} \frac{\Gamma[(n+2)/2]}{\Gamma[(n+3)/2]} \qquad n > -2 \end{aligned} \tag{2.3-17}$$

where $\Gamma(\text{arg})$ is the gamma function of the indicated argument.[1] In the event that $n$ is a positive odd integer, $N(A)$ can be rewritten as

$$N(A) = c_n \frac{n(n-2)(n-4)\cdots(3)}{(n+1)(n-1)(n-3)\cdots(4)} A^{n-1} \qquad n \text{ is an } \textit{odd} \text{ integer} > 1 \tag{2.3-18}$$

If $n$ is a positive even integer, we obtain the following expansion for $N(A)$:

$$N(A) = c_n \frac{4}{\pi} \frac{n(n-2)(n-4)\cdots(2)}{(n+1)(n-1)(n-3)\cdots(3)} A^{n-1} \qquad n \text{ is an } \textit{even} \text{ integer} > 0 \tag{2.3-19}$$

[1] Those properties of the gamma function required for use in Eq. (2.3-17) are

$$\Gamma(k+1) = k! \qquad \text{for integers } k \geq 0$$

$$\Gamma(k+1) = k\Gamma(k) \qquad \text{for arbitrary } k > -1$$

and

$$\Gamma(\tfrac{1}{2}) = \sqrt{\pi} \qquad \Gamma(1) = \Gamma(2) = 1$$

These results can be combined to form the DF for the particular odd polynomial nonlinearity described by

$$y = c_1x + c_2x\,|x| + c_3x^3 + c_4x^3\,|x| + c_5x^5 + \cdots \tag{2.3-20}$$

which is

$$N(A) = c_1 + \frac{8}{3\pi}c_2A + \frac{3}{4}c_3A^2 + \frac{32}{15\pi}c_4A^3 + \frac{5}{8}c_5A^4 + \cdots \tag{2.3-21}$$

A plot of the DF for a one-term odd polynomial nonlinearity appears in Appendix B. For values of $n$ greater than unity, the nonlinear characteristic is of increasing slope with increasing input (*hard*). For values of $n$ less than unity, the characteristic is of the saturating variety (*soft*). This accounts for the behavior of DF magnitude as a function of $A$. As $n$ approaches zero, the odd polynomial characteristic approaches the ideal-relay characteristic; this bound is shown for comparison.

## HARMONIC NONLINEARITY

Error-detecting synchros commonly used in ac servomechanisms are capable of continuous rotation as required to follow constant-angular-velocity command inputs. The gain characteristic of a synchro pair is a sinusoidal function of angular position following error. Thus, for the synchro pair, we may write

$$y = M \sin mx \tag{2.3-22}$$

where $y$ is the ac output amplitude, and $x$ is the input angular-position error. The DF for this harmonic nonlinearity is given by

$$\begin{aligned} N(A) &= \frac{4}{\pi A}\int_0^{\pi/2} y(A \sin \psi) \sin \psi \, d\psi \\ &= \frac{4M}{\pi A}\int_0^{\pi/2} \sin (mA \sin \psi) \sin \psi \, d\psi \\ &= \frac{2MJ_1(mA)}{A} \end{aligned} \tag{2.3-23}$$

where $J_1(mA)$ is the Bessel function of order one for real arguments. A plot of the DF for this nonlinearity in Appendix B indicates regions of $-180°$ phase shift, as well as regions of $0°$ phase shift. Boundaries of each region are given by zero crossings of the Bessel function, $J_1(mA)$.

## HYSTERESIS

Electromagnetic current-actuated relays generally have different pull-in and drop-out input-current values. The nonlinear input-output characteristics

for such relays are, as a consequence, multivalued. A typical characteristic is given in Fig. 2.3-8.

To compute the DF for this characteristic we employ the complex exponential form as follows:

$$\begin{aligned} N(A) &= \frac{2j}{\pi A}\int_0^{\pi} y(A\sin\psi)e^{-j\psi}\,d\psi \\ &= \frac{2j}{\pi A}\left[\int_0^{\psi_1}(-D)e^{-j\psi}\,d\psi + \int_{\psi_1}^{\psi_2} 0\,d\psi + \int_{\psi_2}^{\pi} De^{-j\psi}\,d\psi\right] \\ &= \frac{2D}{\pi A}(e^{-j\psi_1} + e^{-j\psi_2}) \end{aligned} \tag{2.3-24}$$

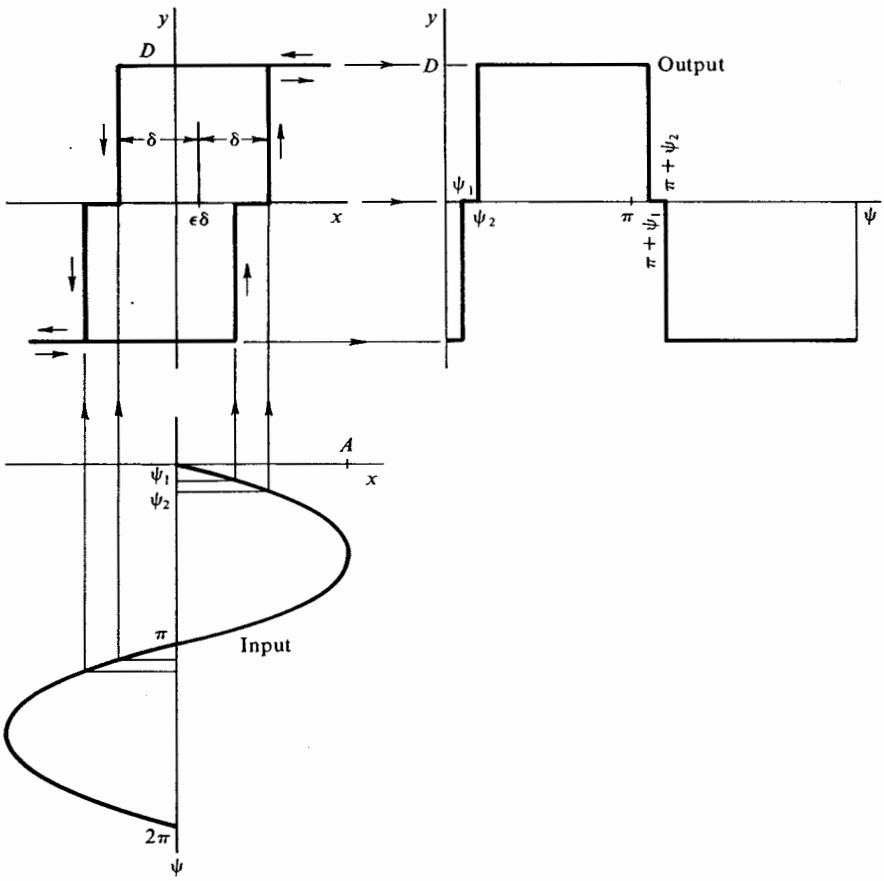


***Figure 2.3-8*** *Hysteresis characteristic with input and output waveforms.*

where $A \sin \psi_1 = \delta(1 - \epsilon)$ or $\psi_1 = \sin^{-1} \frac{\delta}{A} (1 - \epsilon)$

$A \sin \psi_2 = \delta(1 + \epsilon)$ or $\psi_2 = \sin^{-1} \frac{\delta}{A} (1 + \epsilon)$

The DF can be rewritten in terms of the hysteresis characteristic parameters as

$$N(A) = \frac{2D}{\pi A} \left[ \sqrt{1 - \left(\frac{\delta}{A}\right)^2 (1 - \epsilon)^2} + \sqrt{1 - \left(\frac{\delta}{A}\right)^2 (1 + \epsilon)^2} \right] - j \frac{4D\delta}{\pi A^2} \tag{2.3-25}$$

Hence we see for the first time a nonlinearity giving rise to a DF which is complex. Both the magnitude and phase of the DF are functions of $A$. In general, multivalued characteristics will lead to complex DFs.[1] A normalized plot of DF magnitude and phase angle is presented in Appendix B for several values of $\epsilon$.

A special case of the nonlinear characteristic of Fig. 2.3-8 is the *rectangular hysteresis characteristic*, derived by setting $\epsilon = 0$. It is frequently referred to as *toggle* because of its occurrence in mechanical spring-loaded toggle switches. The DF for rectangular hysteresis is given by either of the following forms, derived from Eq. (2.3-24) or (2.3-25) by setting $\epsilon$ to zero.

$$\begin{aligned} N(A) &= \frac{4D}{\pi A} e^{-j \sin^{-1}(\delta/A)} \\ &= \frac{4D}{\pi A} \sqrt{1 - \left(\frac{\delta}{A}\right)^2} - j \frac{4D\delta}{\pi A^2} \end{aligned} \tag{2.3-26}$$

## BACKLASH

Backlash in gearing can be defined as the amount by which a tooth space exceeds the thickness of a mating tooth. A linear force motor engaging its load through a linkage with backlash $b$ is shown in Fig. 2.3-9. The effect of backlash, which is ever-present in geared systems, is almost always destabilizing. For this reason antibacklash (spring-loaded) gearing is often employed. Another approach to circumventing the destabilizing action of backlash in geared systems is to operate the motor with an output velocity bias. This approach is used in the turntable testing of high-quality gyroscopes, for example, where under other circumstances the backlash between motor and turntable could introduce sufficient measurement error to invalidate the testing.

[1] Although there *are* multivalued characteristics for which $n_q(A) = 0$. See Prob. 2-13.

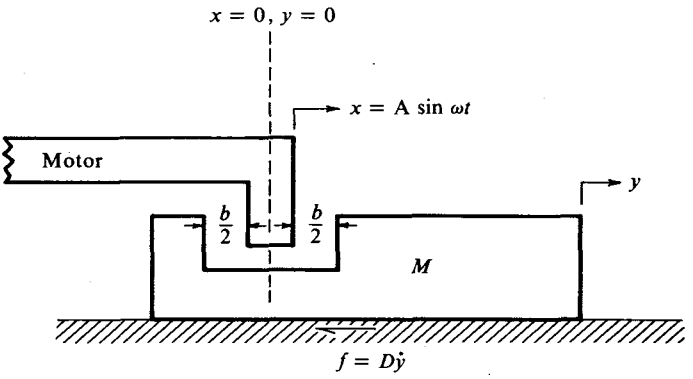


*Figure 2.3-9 Linear motor driving a viscous friction plus inertia load through a linkage with backlash b.*

In order to develop the DF for backlash in the system of Fig. 2.3-9, we consider two limiting cases. In the first of these the friction forces on the load are dominant; this is therefore referred to as *friction-controlled backlash.* In the second the load inertia forces are dominant; this is referred to as *inertia-controlled backlash.* In Sec. 2.4 the more general case, including both friction and inertia forces simultaneously, is treated. In that case a frequency-dependent DF results. In all cases we consider the motor an ideal drive in the sense that it provides a sinusoidal output displacement independent of load force requirements.

**Friction-controlled backlash** In this case we take $M = 0$. A plot of the motor input motion, load output motion, and equivalent backlash characteristic is shown in Fig. 2.3-10. Let us note here that it is not sufficient merely to indicate that a certain amount of backlash is present in a given

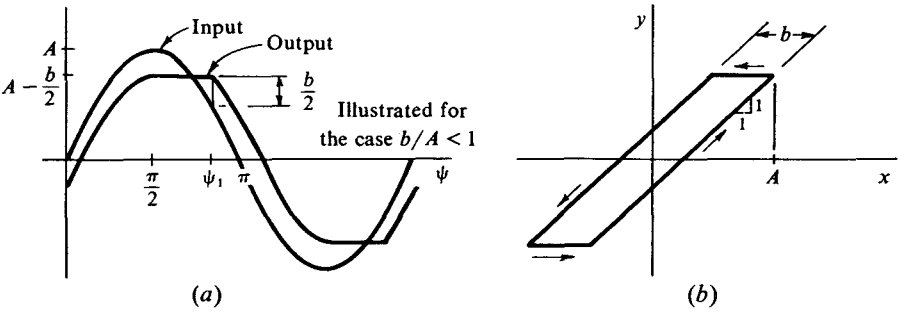


*Figure 2.3-10 (a) Waveforms for friction-controlled backlash. (b) Equivalent backlash characteristic.*

situation; one must further specify the load dynamics in order to derive the equivalent backlash input-output characteristic.

In this case the motor and load are in contact up to the point at which motor velocity reverses. Contact is not reestablished until the backlash is closed on the other side. Bouncing between motor and load is assumed negligible. The DF is computed according to

$$\begin{aligned} N(A) &= \frac{2j}{\pi A}\int_0^{\pi} y(A\sin\psi)e^{-j\psi}\,d\psi \\ &= \frac{2j}{\pi A}\left[\int_0^{\pi/2}\left(A\sin\psi-\frac{b}{2}\right)e^{-j\psi}\,d\psi+\int_{\pi/2}^{\psi_1}\left(A-\frac{b}{2}\right)e^{-j\psi}\,d\psi\right. \\ &\qquad \left.+\int_{\psi_1}^{\pi}\left(A\sin\psi+\frac{b}{2}\right)e^{-j\psi}\,d\psi\right] \\ &= \frac{1}{\pi}\left[\frac{3}{2}\pi-\psi_1-2\left(1-\frac{b}{A}\right)\cos\psi_1+\sin\psi_1\cos\psi_1\right] \\ &\qquad -\frac{j}{\pi}\left[2-2\left(1-\frac{b}{A}\right)\sin\psi_1-\cos^2\psi_1\right] \end{aligned} \tag{2.3-27}$$

The angle $\psi_1$, which defines the point at which the backlash is closed during the negative-velocity part of the cycle, is given by

$$\psi_1 = \pi - \sin^{-1}\left(1-\frac{b}{A}\right) \tag{2.3-28}$$

where $\pi/2 < \psi_1 \leq \pi$ for $0 < b/A \leq 1$; the arcsin is interpreted as an angle in the first quadrant. In terms of $b/A$ the DF can thus be rewritten as

$$N(A) = \frac{1}{\pi}\left[\frac{\pi}{2}+\sin^{-1}\left(1-\frac{b}{A}\right)+\left(1-\frac{b}{A}\right)\sqrt{\frac{2b}{A}-\left(\frac{b}{A}\right)^2}\right]-j\frac{1}{\pi}\left[\frac{2b}{A}-\left(\frac{b}{A}\right)^2\right] \tag{2.3-29}$$

The real part of $N(A)$ can be further rewritten in terms of the saturation function [Eq. (2.3-5)], viz.,

$$\begin{aligned} n_p(A) &= \text{Re}\,[N(A)] \\ &= \frac{1}{2}\left[1+f\left(1-\frac{b}{A}\right)\right] \end{aligned} \tag{2.3-30}$$

in which form its plotting is facilitated since use can now be made of Fig. 2.3-4. The same expression for $N(A)$ results for values $1 < b/A \leq 2$. In that case $\pi < \psi_1 \leq 3\pi/2$, and the arcsin is interpreted as an angle in the fourth quadrant. A plot of the magnitude and phase angle of $N(A)$, calibrated in $b/A$, is given in Fig. 2.3-12.

**Inertia-controlled backlash** In this case we set $D = 0$. Input-output waveforms and the resulting equivalent backlash characteristic are presented in Fig. 2.3-11. Here we see evidence that the specification of backlash is indeed incomplete unless the load description is also included.

At the values $\psi = n\pi$, $n = 0, 1, 2, \ldots$, the motor imparts to the load its maximum velocity, $\dot{x}_{\max} = A\omega = \dot{y}$. Motor-load separation then occurs, and the load coasts with constant velocity until the backlash is closed on the other side. The angle $\psi_1$ at which the backlash is again closed is given by

$$\psi_1 = \sin \psi_1 + \frac{b}{A} \tag{2.3-31}$$

Again we assume bouncing between motor and load to be negligible. The DF is computed according to

$$\begin{aligned} N(A) &= \frac{2j}{\pi A} \int_0^{\pi} y(A \sin \psi) e^{-j\psi}\, d\psi \\ &= \frac{2j}{\pi A} \left[ \int_0^{\psi_1} \left( A\psi - \frac{b}{2} \right) e^{-j\psi}\, d\psi + \int_{\psi_1}^{\pi} \left( A \sin \psi + \frac{b}{2} \right) e^{-j\psi}\, d\psi \right] \\ &= \frac{1}{\pi} (\pi + 2 \sin \psi_1 - \psi_1 - \sin \psi_1 \cos \psi_1) - j \frac{1}{\pi} (1 - \cos \psi_1)^2 \end{aligned} \tag{2.3-32}$$

See Fig. 2.3-12.

If, instead of taking either $M = 0$ or $D = 0$ in each of the above DF calculations, we were to allow $M$ and $D$ to be nonzero, it would still be true that in the limit of increasing input frequency ($\omega \to \infty$) inertia forces would

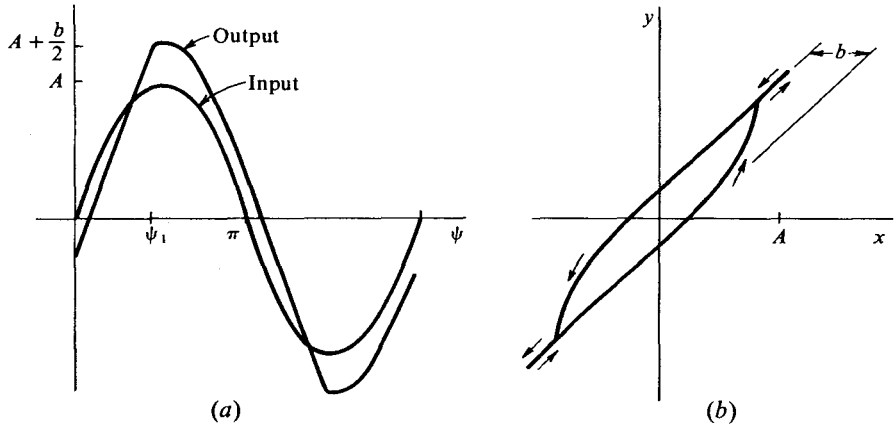


*Figure 2.3-11* (*a*) *Waveforms for inertia-controlled backlash.* (*b*) *Equivalent backlash characteristic.*

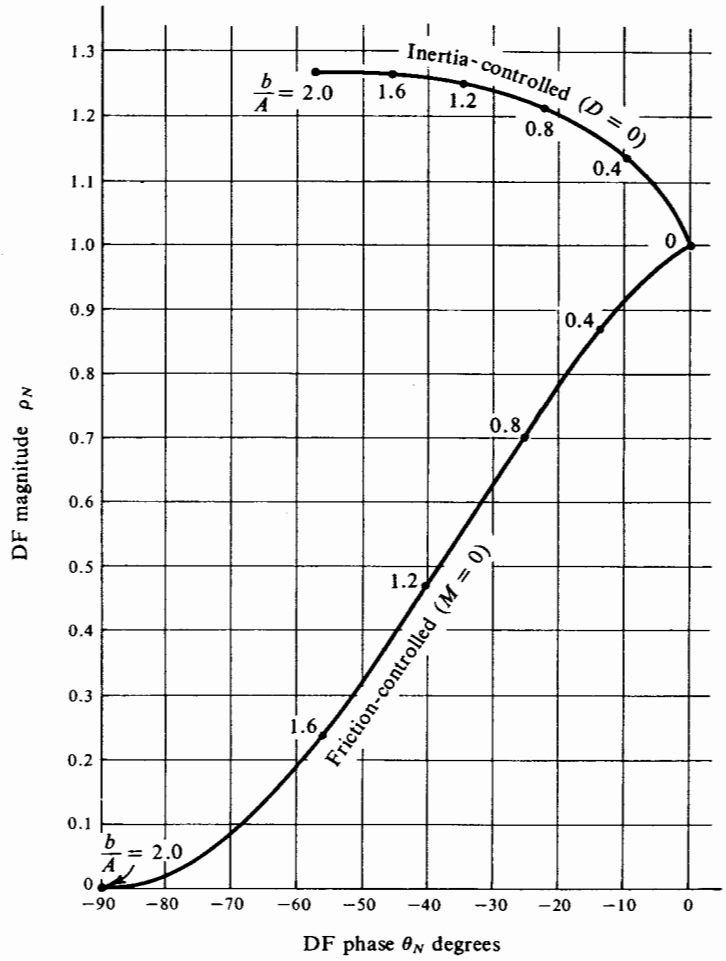


*Figure 2.3-12* *DFs for friction-controlled and inertia-controlled backlash.*

predominate, and in the limit of decreasing input frequency ($\omega \to 0$) friction forces predominate. Hence we might expect the two curves of Fig. 2.3-12 to form the upper and lower bounds of the DF for backlash with both inertia and friction, as input frequency is varied. We indeed observe this behavior in the frequency-dependent-backlash DF calculation of Sec. 2.4.

## HARMONIC GENERATION

The amount by which the output of a sinusoidally forced nonlinearity differs from its first harmonic has been called the *residual*, or *remnant*. Let us

consider the actual output harmonic content associated with several of the nonlinearities whose output first harmonics have been previously determined.

**General piecewise-linear odd memoryless nonlinearity** The ratio of output $k$th-harmonic amplitude to input amplitude is ($\psi_i = \sin^{-1} \delta_i/A$)

$$\begin{aligned}\frac{A_k}{A} &= \frac{4}{\pi A}\int_0^{\pi/2} y(A\sin\psi)\sin k\psi\, d\psi \\ &= \frac{4}{\pi A}\left(\int_0^{\psi_1} y\sin k\psi\, d\psi + \int_{\psi_1}^{\psi_2} y\sin k\psi\, d\psi + \int_{\psi_2}^{\psi_3} y\sin k\psi\, d\psi + \int_{\psi_3}^{\pi/2} y\sin k\psi\, d\psi\right) \\ &= \frac{2}{\pi k}\left[(m_1-m_2)\left(\frac{\sin(k-1)\psi_1}{k-1}+\frac{\sin(k+1)\psi_1}{k+1}\right)\right. \\ &\quad + (m_2-m_3)\left(\frac{\sin(k-1)\psi_2}{k-1}+\frac{\sin(k+1)\psi_2}{k+1}\right) \\ &\quad \left. + (m_3-m_4)\left(\frac{\sin(k-1)\psi_3}{k-1}+\frac{\sin(k+1)\psi_3}{k+1}\right) + m_4\frac{\pi}{2}\right] \end{aligned} \tag{2.3-33}$$

where the values of $y$ for the different intervals of integration are given by Eq. (2.3-9). The result presented above is valid only for $A > \delta_3$, but its alteration to accommodate either larger or smaller regions is straightforward.

**Saturation** The ratio $A_k/A$ for this nonlinear characteristic can be derived from the above result by choosing

$$m_1 = m \qquad m_2 = m_3 = m_4 = 0 \tag{2.3-34}$$

from which it follows that

$$\frac{A_k}{A} = \frac{2m}{\pi k}\left[\frac{\sin[(k-1)\sin^{-1}(\delta/A)]}{k-1} + \frac{\sin[(k+1)\sin^{-1}(\delta/A)]}{k+1}\right] \tag{2.3-35}$$

Harmonic-amplitude ratios are plotted up to the seventh-harmonic term in Fig. 2.3-13.

**Polynomial-type nonlinearities** Consider a one-term $n$th-order polynomial, $n$ odd. The harmonic-amplitude ratio is found according to

$$\begin{aligned}\frac{A_k}{A} &= \frac{4}{\pi A}\int_0^{\pi/2} y(A\sin\psi)\sin k\psi\, d\psi \\ &= \frac{4}{\pi}c_n A^{n-1}\int_0^{\pi/2}\sin^n\psi\sin k\psi\, d\psi \\ &= \frac{c_n A^{n-1}\sin(k\pi/2)\Gamma(n+1)}{2^{n-1}\Gamma[(n+k+2)/2]\Gamma[(n-k+2)/2]} \end{aligned} \tag{2.3-36}$$

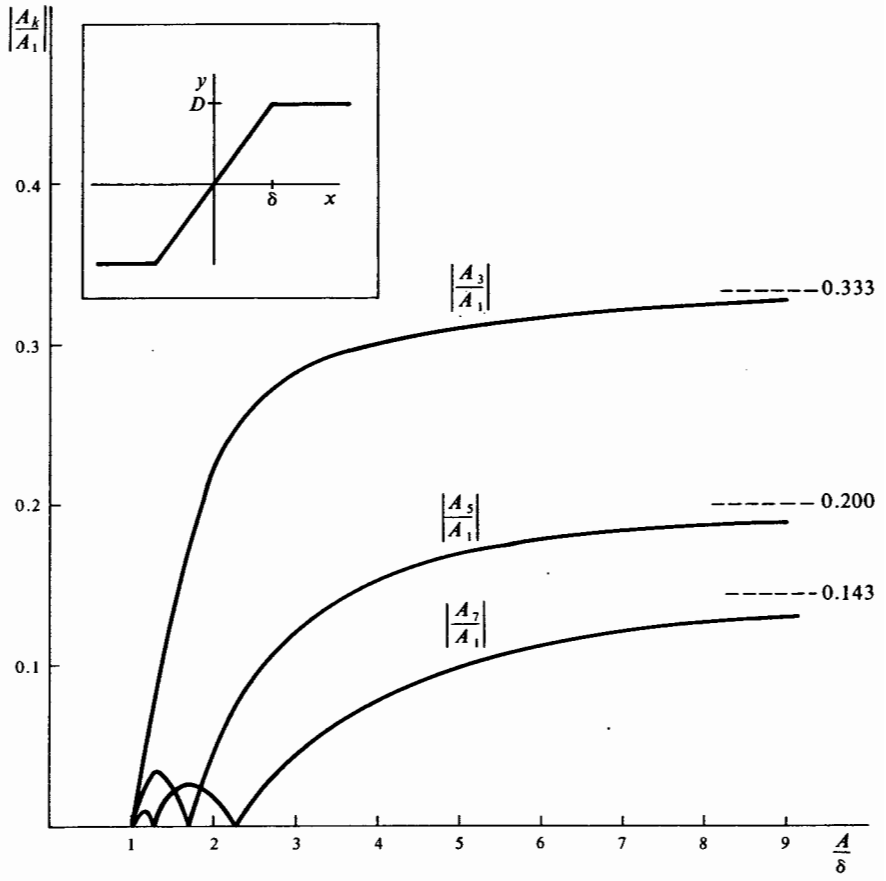


*Figure 2.3-13 Output harmonic content for saturation.*

Results of the related integration for an $n$th-order odd nonlinearity, $n$ even, are identical. Using this expression, the total output harmonic content of many-term polynomial nonlinearities may be built up, one frequency at a time. As expected, $A_k = 0$ for $k$ even. Only odd harmonics exist. When $n$ is odd, we see that all harmonics of order greater than $n$ are zero.

$$A_k = 0 \qquad \text{for all } k > n,\ n \text{ odd} \tag{2.3-37}$$

This can be deduced from Eq. (2.3-36) with the aid of the fact that the value of the gamma function for all negative-integer arguments is infinite. For $n$ even, however, *all* output odd harmonics exist.

**Symmetrical square-law nonlinearity** This characteristic is defined by

$$y = c_2 x\,|x| \tag{2.3-38}$$

Harmonic content is given by

$$\left|\frac{A_k}{A}\right| = \frac{c_2 A}{\Gamma[(4+k)/2]\Gamma[(4-k)/2]} \qquad k \text{ odd} \tag{2.3-39}$$

whence we find

$$\left|\frac{A_3}{A_1}\right| = 0.200 \qquad \left|\frac{A_5}{A_1}\right| = 0.029 \qquad \left|\frac{A_7}{A_1}\right| = 0.010 \tag{2.3-40}$$

**Cubic nonlinearity** Proceeding as before,

$$y = c_3 x^3 \tag{2.3-41}$$

and we find

$$\left|\frac{A_3}{A_1}\right| = 0.33 \qquad \left|\frac{A_5}{A_1}\right| = 0 \qquad \left|\frac{A_7}{A_1}\right| = 0 \tag{2.3-42}$$

**Harmonic nonlinearity** This characteristic is given by

$$y = M \sin mx \tag{2.3-43}$$

Hence the output $k$th harmonic is

$$\begin{aligned} A_k &= \frac{4}{\pi}\int_0^{\pi/2} y(A \sin \psi) \sin k\psi \, d\psi \\ &= \frac{4M}{\pi}\int_0^{\pi/2} \sin (mA \sin \psi) \sin k\psi \, d\psi \\ &= M[1 - (-1)^k]J_k(mA) \end{aligned} \tag{2.3-44}$$

where $J_k(mA)$ is the Bessel function of order $k$. The harmonic-amplitude ratios of interest are

$$\left|\frac{A_3}{A_1}\right| = \left|\frac{J_3(mA)}{J_1(mA)}\right| \qquad \left|\frac{A_5}{A_1}\right| = \left|\frac{J_5(mA)}{J_1(mA)}\right| \qquad \left|\frac{A_7}{A_1}\right| = \left|\frac{J_7(mA)}{J_1(mA)}\right| \tag{2.3-45}$$

These functions are highly oscillatory and reach peaks of up to 70 in the interval $0 < mA \leq 10$. For our present purposes it is sufficient to study the behavior for large $mA$, in which case the Bessel function is well approximated by

$$J_k(mA) \approx \sqrt{\frac{2}{\pi mA}} \cos\left(mA - \frac{k\pi}{2} - \frac{\pi}{4}\right) \tag{2.3-46}$$

Applying this asymptotic representation to the harmonic ratios above, we find

$$\left|\frac{A_3}{A_1}\right| = \left|\frac{A_5}{A_1}\right| = \left|\frac{A_7}{A_1}\right| = 1 \tag{2.3-47}$$

which clearly indicates the presence of substantial harmonic content in the range $mA \gg 1$.

**Rectangular hysteresis** For this characteristic we easily obtain

$$\begin{aligned} |A_k| &= \left|\frac{2j}{\pi}\int_0^{\pi} y(A\sin\psi)e^{-jk\psi}\,d\psi\right| \\ &= \left|\frac{4D}{\pi k}e^{-jk\sin^{-1}(\delta/A)}\right| \\ &= \frac{4D}{\pi k} \qquad k \text{ odd} \end{aligned} \tag{2.3-48}$$

from which the harmonic ratios are

$$\left|\frac{A_3}{A_1}\right| = \frac{1}{3} \qquad \left|\frac{A_5}{A_1}\right| = \frac{1}{5} \qquad \left|\frac{A_7}{A_1}\right| = \frac{1}{7} \tag{2.3-49}$$

**Generalization** For monotonically increasing nonlinear characteristics the $k$th-harmonic output amplitude ratio $|A_k/A_1|$ generally is on the order of $1/k$. Characteristics which are nonmonotonically increasing are apt to possess substantially higher harmonic-amplitude ratios. In most cases, calculation is readily executed.

In the final analysis it is the transfer function of the linear elements of a closed-loop system which emphasizes or deemphasizes loop harmonic content. For those cases in which the loop linear elements contain no resonance peaks at frequencies beyond the nonlinearity input fundamental frequency, DF linearization of a nonlinearity may generally be employed without excessive error due to the presence of unaccounted-for harmonics. This topic will be further pursued in the following chapter.

## 2.4 DF CALCULATION FOR FREQUENCY-DEPENDENT NONLINEARITIES

In this section we examine some methods for dealing with *dynamic* nonlinearities, those for which outputs depend upon inputs and their derivatives. As discussed previously, they are represented as

$$y = y(x,\dot{x}) \tag{2.4-1}$$

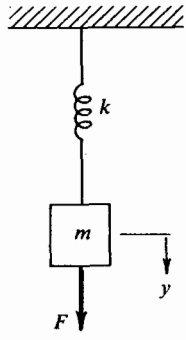


*Figure 2.4-1 Simple linear mass-spring system.*

At any single input frequency a DF magnitude vs. phase-angle plot for varying input amplitude may be constructed, with different such plots belonging to different input frequencies. Thus it will be observed that DFs for dynamic nonlinearities may be generally portrayed by a onefold infinity of graphs, with input frequency as a free parameter.

## LINEAR MECHANICAL SYSTEM

As an example of a very simple system possessing a frequency-dependent DF, consider the single-degree-of-freedom mass-spring system of Fig. 2.4-1. For a sinusoidal force input

$$F = A \sin \omega t \tag{2.4-2}$$

the differential equation of motion of the mass-spring assembly is given by

$$m\ddot{y} + ky = A \sin \omega t \tag{2.4-3}$$

for which the exact *forced* solution is

$$y = \frac{A/m}{k/m - \omega^2} \sin \omega t \tag{2.4-4}$$

Consequently, the DF is given by

$$N(A,\omega) = \frac{1}{A} \frac{A/m}{\omega_n{}^2 - \omega^2} \tag{2.4-5}$$

where $\omega_n{}^2 = k/m$. The amplitude dependence cancels, with the result

$$N(\omega) = \frac{1/m}{\omega_n{}^2 - \omega^2} \tag{2.4-6}$$

which is a function of $\omega$ for fixed system parameters. In fact, the DF presented is *precisely* the linear transfer function of the system from force

input to displacement output. That the DF reduces to the linear transfer function was pointed out earlier in the text.

## BACKLASH WITH A VISCOUS FRICTION PLUS INERTIA LOAD

In its most common form, backlash refers to the play in a pair of otherwise rigidly mounted gears or analogous mechanical linkages. Systems containing gears which have backlash often chatter (limit-cycle) in the absence of an input, a phenomenon which leads to wearing of the gears, and perhaps yet more backlash. Backlash is different from hysteresis (which leads to frequency-independent DFs) in that the nonlinearity output waveform is *not* strictly determined by its input waveform, independent of load properties (friction, inertia, stiffness). For example, if a pure inertia load is driven by a gear train with backlash, the input-output relationship is quite different from that which exists for a pure dashpot load. This behavior was demonstrated in Sec. 2.3, where the limiting cases of friction- and inertia-controlled backlash were studied.

We presently turn our attention to the system of Fig. 2.3-9, where both friction and inertia forces act simultaneously. Typical input and output waveforms are illustrated in Fig. 2.4-2, with the corresponding inertia- and friction-controlled output waveforms for reference. The angle $\psi_s$ denotes

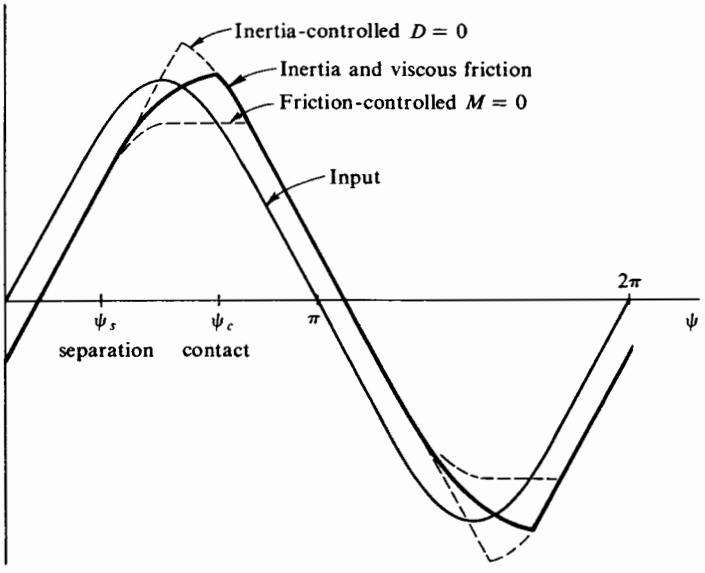


***Figure 2.4-2*** *Input-output waveforms for backlash with viscous friction plus inertia load.*

the point of motor-load separation, which occurs when the motor *decelerates* faster than the load. Using the fact that the velocities of motor and load are identical at separation, one can show that $\psi_s$ is given by

$$\psi_s = \tan^{-1}\frac{1}{\gamma} \tag{2.4-7}$$

where

$$\gamma = \frac{M}{D}\omega \tag{2.4-8}$$

Contact is reestablished when the backlash is again taken up. This occurs at $\psi = \psi_c$, where

$$y(\psi_c) = x(\psi_c) + \frac{b}{2} \tag{2.4-9}$$

which, after insertion of $x(\psi_c)$ and $y(\psi_c)$ in terms of system parameters, can be rewritten in the form

$$\sqrt{1-\gamma^2} - \frac{b}{A} = \sin\psi_c + \frac{\gamma^2 e^{[1/\gamma][\tan^{-1}1/\gamma - \psi_c]}}{\sqrt{1+\gamma^2}} \tag{2.4-10}$$

The in-phase and quadrature components of the DF are found by the now-familiar integration schemes, yielding

$$\begin{aligned} n_p(A,\omega) &= \frac{2}{\pi A}\int_0^{\pi} y(A\sin\psi, A\omega\cos\psi)\sin\psi\, d\psi \\ &= \frac{2\gamma^2}{\pi(1+\gamma^2)}\left[\frac{1+\gamma^2}{2\gamma^2}(\psi_s - \psi_c + \pi + \sin\psi_c\cos\psi_c) + \frac{1}{2\gamma}\right. \\ &\quad + \frac{1}{\gamma}\left(\frac{b}{A} - \sqrt{1+\gamma^2}\right)\left(\frac{1}{\gamma}\cos\psi_c - \sin\psi_c\right) \\ &\quad \left. - \frac{1}{\gamma}\sin^2\psi_c - \sin\psi_c\cos\psi_c\right] \end{aligned} \tag{2.4-11}$$

and

$$\begin{aligned} n_q(A,\omega) &= \frac{2}{\pi A}\int_0^{\pi} y(A\sin\psi, A\omega\cos\psi)\cos\psi\, d\psi \\ &= \frac{-2\gamma^2}{\pi(1+\gamma^2)}\left[1 + \frac{1}{2\gamma^2} + \left(\frac{1-\gamma^2}{2\gamma^2}\right)\sin^2\psi_c\right. \\ &\quad + \frac{1}{\gamma}\left(\frac{b}{A} - \sqrt{1+\gamma^2}\right)\left(\frac{1}{\gamma}\sin\psi_c + \cos\psi_c\right) \\ &\quad \left. + \frac{1}{\gamma}\sin\psi_c\cos\psi_c\right] \end{aligned} \tag{2.4-12}$$

The magnitude and phase of the DF are both functions of $A$ and $\omega$; viz.,

$$\rho_N(A,\omega) = \sqrt{n_p^2(A,\omega) + n_q^2(A,\omega)}$$
$$\theta_N(A,\omega) = \tan^{-1}\frac{n_q(A,\omega)}{n_p(A,\omega)} \tag{2.4-13}$$

A plot of $\rho_N(A,\omega)$ versus $\theta_N(A,\omega)$ for various $A$ and $\omega$ (the latter characterized by $\gamma$) is shown in Appendix B. The whole family of DF loci, as expected, are contained between the curves for the inertia- and friction-controlled backlash cases. Unlike the friction-controlled backlash nonlinearity, the response of inertia-controlled backlash need not be zero for all $A < b/2$. In fact, the DF can be defined for all $A > b/3.72$. Beyond this point, in the direction of decreasing $A$, both subharmonics and aperiodic responses occur. Correspondingly, all intermediate cases shown can be extended somewhat to values of $b/A$ in excess of 2.0, but less than 3.72. Studies of this extension, as well as the cases of backlash with load inertia and coulomb friction, both with zero and nonzero input-velocity biases, are available in the literature (Refs. 11, 16, 44, 46, 52).

## NONLINEAR CLEGG INTEGRATOR

The Clegg integrator (Refs. 5, 33) represents an attempt to synthesize a nonlinear circuit possessing the amplitude-frequency characteristic of a linear integrator while avoiding the 90° phase lag associated with the linear transfer function. Clearly, no linear circuit can accomplish this objective since the linear integrator is itself a minimum-phase network.

A functional diagram of the Clegg integrator, which switches on input zero crossings, is illustrated in Fig. 2.4-3*a*. Basically, operation consists of the input being gated through one of two integrators (the output of the other is simultaneously reset) in accordance with zero-crossing detector (ZCD) commands. Implementation of this integrator, including gates and ZCD, can be effected with four diodes, four $RC$ networks, and two operational amplifiers (Ref. 5). Input and output waveforms are shown in Fig. 2.4-3*b*. In the interval $0 < \psi < \pi$, the output is ($\psi = \omega t$)

$$y(\psi) = \int_0^{\psi/\omega} x\, d\left(\frac{\psi}{\omega}\right)$$
$$= \frac{1}{\omega}\int_0^{\psi} A \sin\psi\, d\psi$$
$$= \frac{A}{\omega}(1 - \cos\psi) \tag{2.4-14}$$

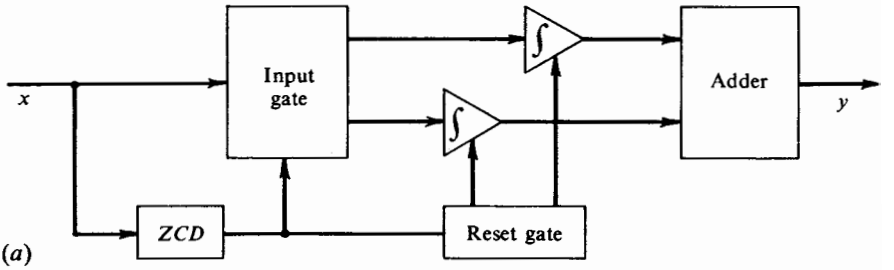


(a)

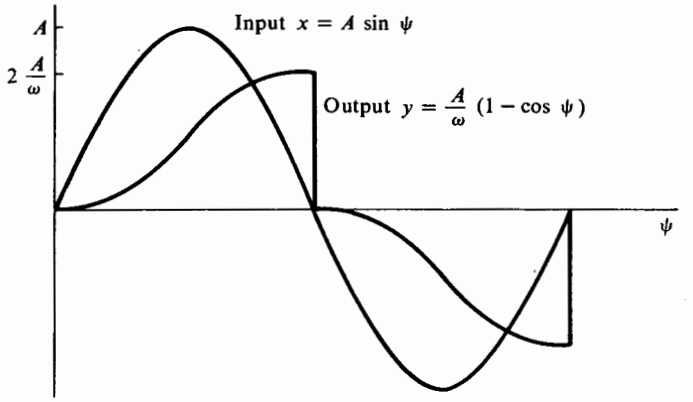


(b)

***Figure 2.4-3*** *(a) Nonlinear Clegg integrator. (b) Associated input-output waveforms.*

The DF is thus given by

$$N(A,\omega) = \frac{2j}{\pi A}\int_0^{\pi} y(A\sin\psi, A\omega\cos\psi)e^{-j\psi}\,d\psi$$

$$= \frac{2j}{\pi A}\int_0^{\pi} \frac{A}{\omega}(1-\cos\psi)e^{-j\psi}\,d\psi$$

$$= \frac{4}{\pi\omega}\left(1 - j\frac{\pi}{4}\right) \tag{2.4-15}$$

and it is evident that the (in this case) undesired dependence of the DF upon input amplitude has been successfully avoided, with the result

$$N(\omega) = \frac{1}{\omega}\sqrt{1+\left(\frac{4}{\pi}\right)^2}\,e^{-j\tan^{-1}(\pi/4)}$$

$$= \frac{1.619}{\omega}\,e^{-j38.15^\circ} \tag{2.4-16}$$

This DF has associated with it approximately 52° less phase lag than that for the linear integrator. Its merit as a system compensation network from the point of view of loop stability is thus apparent.

Harmonic content in the sinusoidally forced output of this nonlinear integrator follows directly from the observation that the output is the sum of a square wave of amplitude $A/\omega$ and a negative cosine wave of amplitude $A/\omega$, both of equal period. The output $k$th harmonic is therefore due entirely to the square-wave portion

$$A_k = \frac{4A}{\pi\omega k} \qquad k \text{ odd} \tag{2.4-17}$$

and the harmonic-amplitude ratios of interest are

$$\left|\frac{A_3}{A_1}\right| = \frac{1}{3} \qquad \left|\frac{A_5}{A_1}\right| = \frac{1}{5} \qquad \left|\frac{A_7}{A_1}\right| = \frac{1}{7} \tag{2.4-18}$$

which are typical, as previously noted.

## FREQUENCY-INDEPENDENT DFs FROM FREQUENCY-DEPENDENT NONLINEARITIES

We have seen that the frequency-dependent DF can be treated by a simple extension of the basic DF concept. The result of this approach is a family of DF loci, perhaps with frequency as a convenient family parameter. Although it is true that analysis can now proceed within this framework, one additional approach is well worth consideration. The intent of this method is the divorce of linear frequency-dependent and nonlinear amplitude-dependent parts of an otherwise amplitude- and frequency-dependent nonlinear element. Although such a division cannot always be effected, when it can, the resultant nonlinear element will be far simpler to handle. In particular, the DF associated with the nonlinearity will be frequency-independent (Ref. 3).

Consider the four-terminal nonlinear $RC$ network of Fig. 2.4-4*a*. For the purpose of demonstration we shall work under the condition that the nonlinear network must be treated as shown and that no physical reorganization within some larger system is possible. Given the voltage-current characteristic $e_2 = N_1(i_2)$ of the network diode, we may proceed to manipulate system variables to obtain the desired end result. Laplace transform notation is most convenient in this endeavor. In this form the equations governing system behavior are

$$\begin{aligned} E_1(s) - E_2(s) &= RI_1(s) \\ I_1(s) - I_2(s) &= CsE_2(s) \\ e_2 &= N_1(i_2) \end{aligned} \tag{2.4-19}$$

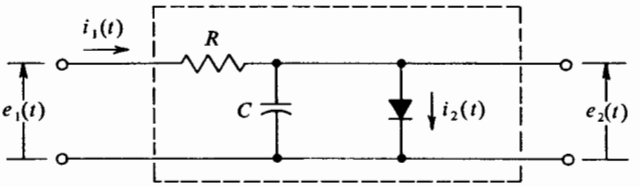


(*a*) *RC* network with diode rectifier

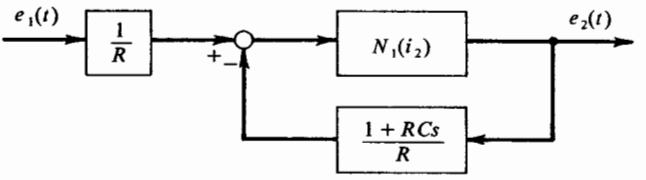


(*b*) Block diagram of equivalent system

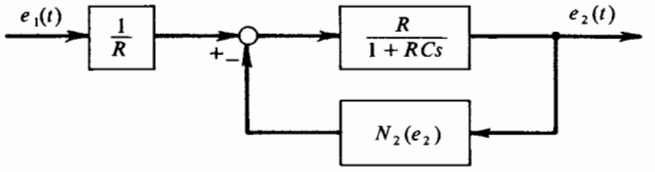


(*c*) Another block diagram of equivalent system

***Figure 2.4-4*** *Frequency-dependent nonlinearity and two equivalent block-diagram representations.*

which may easily be represented by block diagram, as in Fig. 2.4-4*b*. This block diagram contains only linear frequency-dependent elements and nonlinear frequency-independent elements. The desired separation has been accomplished since the isolated nonlinear part of the block diagram is frequency-independent. If the nonlinear *RC* network were part of a larger and otherwise linear system, the linear feedback branch of this network could be associated with the rest of the system to yield a final block diagram in which there would exist a single amplitude-dependent nonlinearity plus other purely linear elements. Analytic studies of this system would be in terms of a frequency-independent DF, considerably more convenient than equivalent studies using the corresponding frequency-dependent DF.

For the above example it is also possible to generate another useful block diagram. This new configuration contains a frequency-independent nonlinearity in the feedback path, which happens to be the inverse of the

nonlinearity representation given before, namely, $i_2 = N_2(e_2)$. Figure 2.4-4*c* depicts this arrangement. Stout (Ref. 50) has shown that any two-part system containing a single explicit nonlinearity can always be reduced to four topologically identical and mathematically equivalent block diagrams. In these diagrams the nonlinear element may appear as either a forward or feedback block, with its input and output in either a normal or reversed cause-effect relationship.

## DF CALCULATION FOR IMPLICIT DYNAMIC NONLINEARITIES

Many nonlinearities are best described in terms of input-output differential equations. This is as opposed to some explicit dynamical description, for example. Under this circumstance the nonlinearity output waveform is not generally available directly in terms of its input, as has previously been assumed. The *implicit* dynamical relationship between input and output must therefore be dealt with by some special means. In order to demonstrate one useful method of approach, we compute the DF for the dynamic nonlinearity described by

$$\ddot{y} + 3y^2\dot{y} + y = x \tag{2.4-20}$$

where $x$ and $y$ are the nonlinearity input and output, respectively. To find $y(t)$ in response to the harmonic input

$$x = A \sin (\omega t + \theta) \tag{2.4-21}$$

one must possess the general solution of Eq. (2.4-20). Generally speaking, the solutions to nonlinear differential equations are unknown. Rather than obtain $y(t)$, and thus derive the DF by performing the usual Fourier expansion, we now are forced to seek an alternative approach. An artifice frequently worthwhile is to assume for the form of the nonlinearity output

$$y = Y \sin \omega t \tag{2.4-22}$$

and to solve for the sinusoidal input which results in this output. First-harmonic approximation allows execution of this method.

Inserting Eqs. (2.4-21) and (2.4-22) into (2.4-20), we get

$$-\omega^2 Y \sin \omega t + 3\omega Y^3 \sin^2 \omega t \cos \omega t + Y \sin \omega t = A \sin (\omega t + \theta) \tag{2.4-23}$$

The second term on the left-hand side may be expanded into first- and third-harmonic portions, viz.,

$$\sin^2 \omega t \cos \omega t = \tfrac{1}{4} \cos \omega t - \tfrac{1}{4} \cos 3\omega t \tag{2.4-24}$$

Dropping the third-harmonic term, Eq. (2.4-23) becomes

$$(1 - \omega^2) Y \sin \omega t + \tfrac{3}{4}\omega Y^3 \cos \omega t = A \sin (\omega t + \theta) \tag{2.4-25}$$

Collating coefficients of sin $\omega t$ and cos $\omega t$ yields the following equations in $A$, $Y$, $\theta$:

$$\begin{aligned}(1 - \omega^2)Y &= A\cos\theta \\ \tfrac{3}{4}\omega Y^3 &= A\sin\theta\end{aligned} \tag{2.4-26}$$

Equations (2.4-26) may be simultaneously solved to yield $\theta(A,\omega)$, $Y(A,\omega)$.

$$(1 - \omega^2)^2 Y^2 + (\tfrac{3}{4}\omega Y^3)^2 = A^2 \tag{2.4-27}$$

$$\theta = \tan^{-1}\left(\frac{3}{4}\frac{\omega Y^2}{1 - \omega^2}\right) \tag{2.4-28}$$

Equation (2.4-27) is an implicit relationship for $Y(A,\omega)$, which, once obtained, may be used to find $\theta(A,\omega)$ given explicitly by Eq. (2.4-28). The first-harmonic gain of the nonlinearity is given by

$$\begin{aligned}N(A,\omega) &= \frac{Y(A,\omega)}{A}\, e^{-j\theta(A,\omega)} \\ &= \rho_N(A,\omega)e^{j\theta_N(A,\omega)}\end{aligned} \tag{2.4-29}$$

Equations (2.4-27) and (2.4-28) may be rewritten in terms of $\rho_N$ and $\theta_N$.

$$\begin{aligned}\rho_N{}^6 + \left(\frac{4}{3}\frac{1 - \omega^2}{\omega A^2}\right)^2 \rho_N{}^2 - \left(\frac{4}{3\omega A^2}\right)^2 &= 0 \\ \theta_N = -\tan^{-1}\left(\frac{3}{4}\frac{\omega\rho_N{}^2 A^2}{1 - \omega^2}\right)\end{aligned} \tag{2.4-30}$$

Thus the frequency-dependent DF has been determined. These results are identical with those presented elsewhere (Ref. 39), the same nonlinear equation in that instance treated by a method of Stoker (Ref. 49). Observe that the exact output first harmonic has not been calculated; rather, an approximation to it has been arrived at. Better approximations can be generated by assuming a more complete description of $y$ in Eq. (2.4-22); however, the labor entailed rapidly increases.

## EXTENSIONS OF THE DF CONCEPT

Another method for dealing with implicit dynamical nonlinearities has been developed by Klotter (Ref. 26), who replaces the Fourier harmonic concept of the DF with a corresponding "Hamilton harmonic" concept. In particular, he chooses the nonlinearity output amplitude and phase so as to minimize the integral whose Euler equation coincides with the given differential equation. This process is somewhat analogous to minimizing the mean-squared error in conventional DF formulation by selecting the Fourier series

representation of a nonlinearity output [Eq. (2.2-23)]. One significant difference between the two methods is that the Fourier coefficients are fixed, independent of the degree of approximation employed, whereas the Hamilton harmonics depend in some way upon rejected higher harmonics (the residual). DFs generated by both methods are reported to show first-harmonic amplitude differences of the order of 10 percent.

It is possible to propose any number of other linearization schemes based upon a sinusoidal input. For example, the equivalent gain could be chosen to minimize the average approximation error or absolute magnitude of the error rather than mean-squared error as in DF formulation. Although the above-mentioned alternatives do not appear to have any advantage over the DF, an "rms DF" proposed by Gibson and Prasanna-Kumar (Ref. 12) shows some promise in application to systems with odd single-valued nonlinearities. It is defined by

$$N_{\text{rms}}(A) = \left[ \frac{\int_0^{2\pi} [y(A \sin \psi)]^2 \, d\psi}{\int_0^{2\pi} (A \sin \psi)^2 \, d\psi} \right]^{\frac{1}{2}} \tag{2.4-31}$$

That is, the equivalent sinusoidal output of the nonlinearity is chosen to have the same rms value as the actual output. Using the notation of Fig. 2.2-1, it is readily demonstrated that Eq. (2.4-31) can be written as (odd nonlinearity)

$$N_{\text{rms}}(A) = \frac{\sqrt{A_1^2 + A_3^2 + A_5^2 + A_7^2 + \cdots}}{A}$$

Rankine and D'Azzo have proposed a "corrected conventional DF" based upon a truncated version of the rms DF, as follows:

$$N_{\text{ccDF}}(A) = \frac{\sqrt{A_1^2 + A_3^2}}{A} \tag{2.4-32}$$

In application to the study of a wide variety of systems, the corrected conventional DF was found to be consistently more accurate than either the DF or rms DF, although all results were, in fact, quite good (Ref. 43).

Another mechanism for studying the limit cycle behavior of certain nonlinear systems is the "elliptic describing function" (Ref. 24). It is particularly interesting in that the limit cycle waveshape is determined *after* the amplitude and frequency have been found. This differs from other DF methods wherein the waveshape is specified a priori. However, the computation associated with the elliptic-describing-function method and its practical restriction to single-valued odd static nonlinearities appear to rule it out as a generally useful analytical tool.

For the remainder of this and the following two chapters we confine our consideration to the conventional DF.

## 2.5 SYNTHESIS OF DFs

The DF for a complex nonlinearity can be synthesized by vector addition of the DFs for a group of similar nonlinearities whose *parallel* combination has the identical input-output characteristic. The method relates to vector addition of sinusoids and is exact within its own framework. Series-connected nonlinearities do not support the same generalizations. These cases are treated in what follows.

Consider $n$ nonlinearities $N_1, N_2, \ldots, N_n$ in parallel such that their total output $y(x)$ is

$$\begin{aligned} y(x) &= y_1(x) + y_2(x) + \cdots + y_n(x) \\ &= \sum_{i=1}^{n} y_i(x) \end{aligned} \tag{2.5-1}$$

It then follows that the DF for the composite nonlinearity is given by

$$\begin{aligned} N(A) &= \frac{j}{\pi A} \int_0^{2\pi} \left[ \sum_{i=1}^{n} y_i(A \sin \psi) \right] e^{-j\psi}\, d\psi \\ &= \frac{j}{\pi A} \sum_{i=1}^{n} \int_0^{2\pi} y_i(A \sin \psi) e^{-j\psi}\, d\psi \\ &= \sum_{i=1}^{n} N_i(A) \end{aligned} \tag{2.5-2}$$

Thus the DF for the composite nonlinearity is the sum of DFs for the individual nonlinearities comprising the composite nonlinearity. Since, in general, the DF for the $i$th nonlinearity is a complex quantity, Eq. (2.5-2) represents a vector addition. In the case of frequency- and amplitude-dependent elemental nonlinearities, the DF for a parallel combination is given as

$$N(A,\omega) = \sum_{i=1}^{n} N_i(A,\omega) \tag{2.5-3}$$

by direct analogy with Eq. (2.5-2). Once again the sum implies a vector addition.

One may assess the harmonic content of the composite nonlinearity output merely by performing appropriate vector additions on the individual harmonic terms of like frequency, again in a manner completely analogous to that of Eq. (2.5-2).

An example of the synthesis of a complex nonlinearity from simpler forms is the construction of the nonrectangular hysteresis-type nonlinearity (Fig. 2.5-1*a*) from the rectangular-hysteresis and linear-gain functions (Fig.

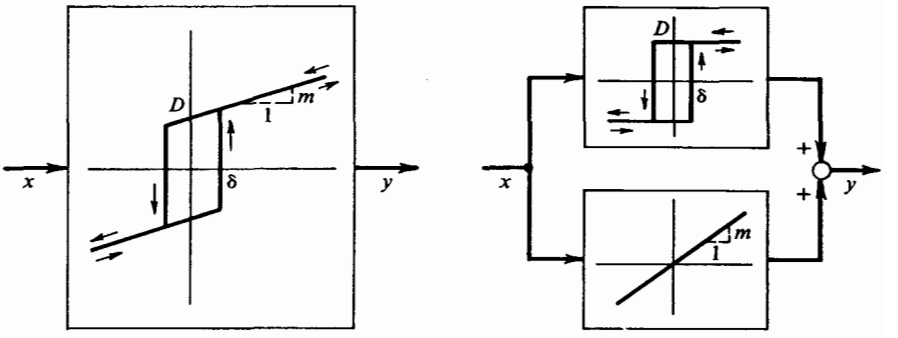


***Figure 2.5-1*** *Synthesis of a simple hysteresis characteristic (a) from the elemental forms of rectangular hysteresis and linear gain (b).*

2.5-1*b*). By executing two simple sketches the doubtful reader may convince himself of the validity of this maneuver, observing that the sinusoidally forced output of the simple nonrectangular-hysteresis element and the sum of sinusoidally forced outputs of the rectangular-hysteresis and linear-gain elements are identical. Accordingly, we have [Eq. (2.3-26)]

$$N(A) = \underset{\substack{\text{rectangular}\\ \text{hysteresis}}}{N_1(A)} + \underset{\substack{\text{linear}\\ \text{gain}}}{N_2(A)}$$

$$= \frac{4D}{\pi A} e^{-j \sin^{-1}(\delta/A)} + m \tag{2.5-4}$$

In terms of a real and imaginary part, or a magnitude and phase angle, the composite DF may be directly rewritten as follows:[1]

$$N(A) = \left[\frac{4D}{\pi A}\sqrt{1 - \left(\frac{\delta}{A}\right)^2} + m\right] - j\left(\frac{4D\delta}{\pi A^2}\right)$$

$$= \left[\left(\frac{4D}{\pi A}\right)^2 + m^2 + \frac{8Dm}{\pi A}\sqrt{1 - \left(\frac{\delta}{A}\right)^2}\right]^{\frac{1}{2}}$$

$$\times \exp\left\{-j \tan^{-1}\left[\frac{4D(\delta/A)}{4D\sqrt{1 - (\delta/A)^2} + \pi A m}\right]\right\} \tag{2.5-5}$$

[1] The expression giving the real and imaginary parts of $N(A)$ is least cumbersome of the two presented in Eq. (2.5-5). Since this is generally the case for complex nonlinearities with memory, Appendix B lists DFs in terms of their real and imaginary parts.

The harmonics generated by this composite nonlinearity are given by Eq. (2.3-49) and are due entirely to rectangular hysteresis, the linear gain generating no output harmonic content whatever.

Now consider the case of series-connected nonlinearities. To demonstrate the complexity of this situation, Fig. 2.5-2 illustrates the series connection of friction-controlled backlash followed by a limiter with dead zone. The two possible overall characteristics resulting for various ranges of $A$ are also presented. It is at once evident that the decomposition, or synthesis procedure, is all but hopeless. No simple results exist comparable with the case of parallel-connected nonlinearities.

The question arises as to whether any simplified solution for the DF exists. In partial answer to this question, Gronner (Ref. 19) has shown that the exact DF for friction-controlled backlash followed by dead zone and an approximate DF computed directly by *multiplication* of the DFs of the individual nonlinearities compare quite well. Such a procedure implicitly assumes that the output of the first nonlinearity may in some sense be considered sinusoidal, in order to utilize the DF of the second nonlinearity in subsequent overall approximate DF calculation. This could be the case if, for example, the original nonlinearities were separated by a linear filter which, during analysis,

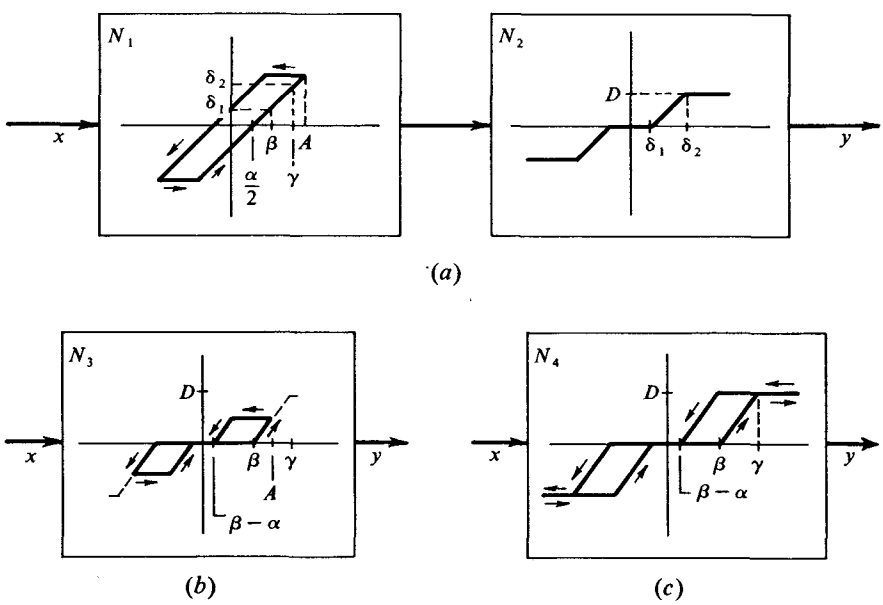


***Figure 2.5-2*** *Series-connected nonlinearities. Elemental froms (a) and the corresponding overall characteristics for (b) $\beta < A < \gamma$ and (c) $A > \gamma$.*

was associated with the first nonlinearity. Unfortunately, generalizations regarding expected accuracy of DF calculation using this procedure for a variety of nonlinearity combinations are not available.

## 2.6 TECHNIQUES FOR APPROXIMATE CALCULATION OF THE DF

Given any nonlinear characteristic, the corresponding DF can theoretically be evaluated using the techniques of previous sections. However, in practice, nonlinear characteristics are often known only by measurement of a physical system, precise analytic relationships remaining unknown. The DF can still be evaluated following an analytic curve fit of the experimentally derived characteristic, but time required to effect this curve fit and subsequent DF calculation may be unwarranted, considering that analysis following derivation of the DF is of an approximate nature. In fact, even given a nonlinear characteristic of precise analytical definition, an approximate DF calculation can often be justified on the grounds of approximate ultimate analysis. Furthermore, exact calculation can be tedious and lengthy.

To begin with, it may be possible to evaluate the DF experimentally. If a system nonlinearity can be isolated and excited with a sine wave of known amplitude and frequency, the application of a harmonic analyzer to the nonlinearity output directly yields all information necessary for DF specification. Instruments have been designed which automatically compute the frequency response of nonlinear systems based upon measurement of the evoked response to harmonic excitation (Refs. 4, 21, 57). Here we concern ourselves with approaches which can be executed with pencil and paper, starting at the point just after determination of the nonlinear characteristic. Thus we seek approximate methods for expediting hand calculation of the DF.

The most straightforward approach to graphic DF evaluation, starting with the nonlinear characteristic, is point-by-point derivation of the nonlinearity output waveform and harmonic analysis of it by direct area measurements (such as discussed in Ref. 8). Clearly, this is not the best manner of calculation. It would be more desirable, for example, to work directly with the nonlinear characteristic, without ever having to graph the actual output waveform. Several methods of computation having this virtue are considered. Let us restrict our attention to odd static symmetric nonlinearities.

### PIECEWISE-LINEAR APPROXIMATION

The first approach deserving of mention simply prescribes an $n$-segment piecewise-linear fit to any given nonlinear characteristic. The DF for the

resultant nonlinear characteristic is either given by the general formula of Eq. (2.3-10), if that characteristic is memoryless, or can be derived by the methods of Sec. 2.3, if the characteristic possesses memory. Three or four segments per quadrant usually result in acceptable accuracy. The extension of this point of view to a piecewise-polynomial approximation is evident.

## ANALYTIC SOLUTION OF THE DF INTEGRAL

A basis for the approximate analytic evaluation of the DF consists in the development of an approximate expansion of the exact DF integral formulation (Refs. 36, 51). Consider the case of a single-valued characteristic, for which the DF is given by

$$N(A) = \frac{2}{\pi A} \int_{-\pi/2}^{\pi/2} y(A \sin \psi) \sin \psi \, d\psi \tag{2.6-1}$$

Under the transformation

$$u = \sin \psi \qquad du = \cos \psi \, d\psi \tag{2.6-2}$$

Eq. (2.6-1) can be rewritten as

$$N(A) = \frac{2}{\pi A} \int_{-1}^{1} y(Au) \frac{u \, du}{\sqrt{1 - u^2}} \tag{2.6-3}$$

The evaluation of a related integral is

$$\int_{-1}^{1} \frac{g(u) \, du}{\sqrt{1 - u^2}} \approx \frac{\pi}{6} [g(1) + g(-1) + 2g(0.5) + 2g(-0.5)] \tag{2.6-4}$$

This result can be demonstrated as exact for the case of $g(u)$ as the series expansion

$$g(u) = a_2u^2 + a_3u^3 + a_4u^4 + a_5u^5$$

which, by virtue of the required connecting identity

$$g(u) = uy(Au) \tag{2.6-5}$$

implies a nonlinear characteristic of the form

$$y(u) = b_1u + b_2u^2 + b_3u^3 + b_4u^4$$

From Eqs. (2.6-4) and (2.6-5) it follows that the DF is given by

$$N(A) \approx \frac{1}{3A} \left[ y(A) - y(-A) + y\left(\frac{A}{2}\right) - y\left(-\frac{A}{2}\right) \right] \tag{2.6-6}$$

For characteristics which are odd, this reduces to

$$N(A) \approx \frac{2}{3A}\left[y(A) + y\left(\frac{A}{2}\right)\right] \tag{2.6-7}$$

The significance of these simple results can be demonstrated by example.

**Example 2.6-1** (*a*) Find the DF for the odd polynomial characteristic

$$y(x) = c_1x + c_2x|x| + c_3x^3 + c_4x^3|x| + c_5x^5$$

Applying the formula obtained above, we get

$$N(A) \approx c_1 + \tfrac{8}{6}c_2A + \tfrac{3}{4}c_3A^2 + \tfrac{17}{24}c_4A^3 + \tfrac{11}{16}c_5A^4$$

The exact DF [Eq. (2.3-21)] is repeated for convenience:

$$N(A) = c_1 + \frac{8}{3\pi}c_2A + \frac{3}{4}c_3A^2 + \frac{32}{15\pi}c_4A^3 + \frac{5}{8}c_5A^4$$

In analyzing the result, first observe that the terms in $c_1$ and $c_3$ are exact. This is expected because of the formulation of $g(u)$. The terms in $c_2$ and $c_4$ are in error by less than 4 percent. Since $g(u)$ does *not* imply any odd terms of even power in the nonlinear characteristic, these results are encouraging. The term in $c_5$ is in error by 10 percent.

(*b*) Find the DF for an ideal-relay characteristic

$$y(x) = D\frac{x}{|x|}$$

By Eq. (2.6-7) we get the result

$$N(A) \approx \frac{4D}{3A}$$

The exact result is

$$N(A) = \frac{4D}{\pi A}$$

from which we observe that only a 4.5 percent error has been incurred in using the approximate DF calculation. This excellent result can be explained in part by noting that the same approximate DF formulation as in Eqs. (2.6-6) and (2.6-7) is obtained for characteristics given by

$$y(u) = \frac{b_{-1}}{u} + b_0 + b_1u + b_2u^2$$

where the leading term is seen to be discontinuous (more precisely, *undefined*) at the origin. Again the result is encouraging.

Another approximation to $N(A)$, derived in a manner similar to that presented above and yielding even better accuracies, is (odd nonlinearity, see Ref. 46)

$$N(A) \approx \frac{1}{3A}\left[y(A) + y\left(\frac{A}{2}\right) + \sqrt{3}y\left(\frac{\sqrt{3}A}{2}\right)\right] \tag{2.6-8}$$

By application to Example 2.6-1 it is verified that approximation errors using

this result are smaller than those previously obtained. Odd polynomials of odd exponent up to 9 may be treated with zero error. Calculation of the DF for saturation by either Eq. (2.6-7), the first approximation, or (2.6-8), the second approximation, yields errors of less than 5 percent, the latter with smaller error over most of the range considered. Approximately computed DFs for saturation, increasing gain, relay with dead zone, and harmonic nonlinearities are shown with their exact counterparts in Fig. 2.6-1.

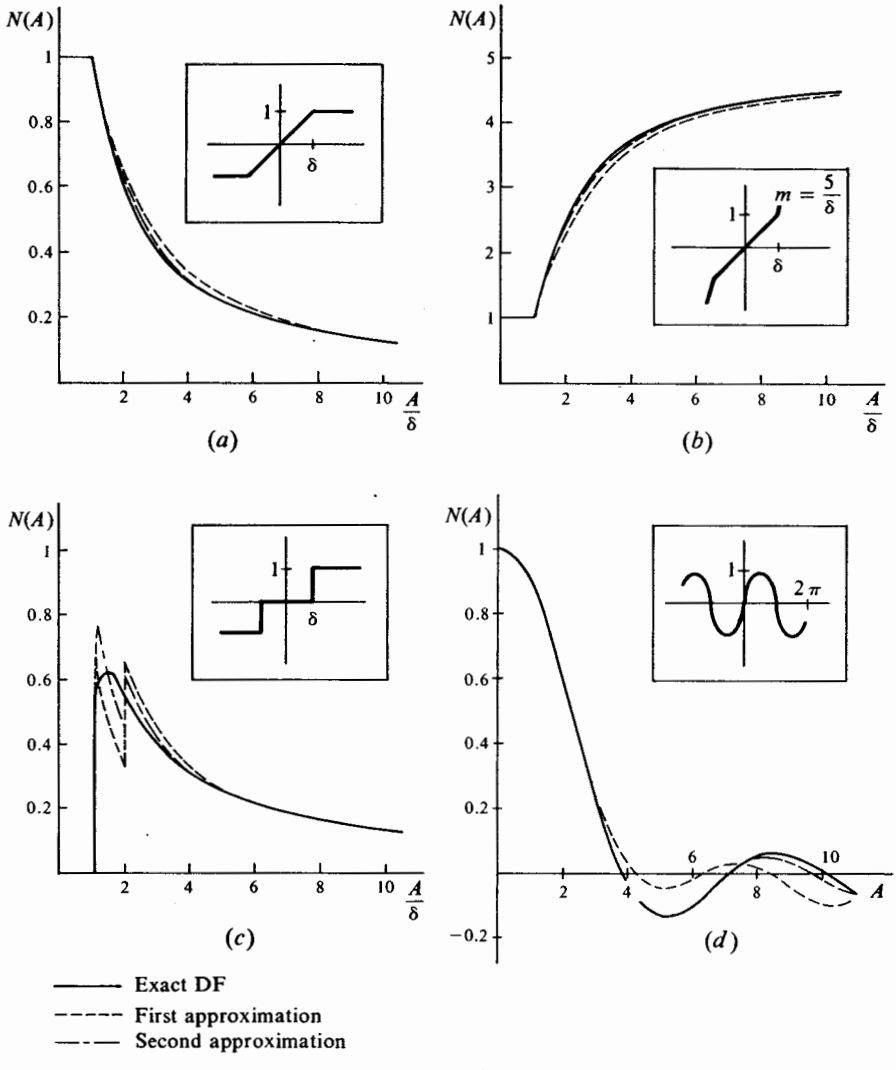


*Figure 2.6-1* *Approximately computed DFs for (a) saturation, (b) increasing gain, (c) relay with dead zone, and (d) harmonic nonlinearity.*

The approximate DF solution presented in this section has been generalized to encompass arbitrary nonlinear characteristics with memory. Allowing the double-valued $y(x)$ to be separated into $y_1(x)$, valid when $x$ is decreasing, and $y_2(x)$, valid when $x$ is increasing, it has been shown (Ref. 38) that

$$n_p(A) \approx \frac{1}{6A}\left[y_1(A) + y_2(\dot{A}) - y_1(-A) - y_2(-A) + y_1\left(\frac{A}{2}\right) + y_2\left(\frac{A}{2}\right) - y_1\left(-\frac{A}{2}\right) - y_2\left(-\frac{A}{2}\right)\right] \quad (2.6\text{-}9a)$$

and

$$n_q(A) \approx -\frac{1}{6\pi A}\left[y_1(A) - y_2(A) + 4y_1\left(\frac{A}{2}\right) - 4y_2\left(\frac{A}{2}\right) + 2y_1(0) - 2y_2(0) + y_1(-A) - y_2(-A) + 4y_1\left(-\frac{A}{2}\right) - 4y_2\left(-\frac{A}{2}\right)\right] \quad (2.6\text{-}9b)$$

For symmetric characteristics $[y_1(x) = -y_2(-x)]$ these expressions become

$$n_p(A) \approx \frac{1}{3A}\left[y_1(A) + y_2(A) + y_1\left(\frac{A}{2}\right) + y_2\left(\frac{A}{2}\right)\right] \quad (2.6\text{-}10a)$$

and

$$n_q(A) \approx -\frac{1}{3\pi A}\left[y_1(A) - y_2(A) + 4y_1\left(\frac{A}{2}\right) - 4y_2\left(\frac{A}{2}\right) + 2y_1(0)\right] \quad (2.6\text{-}10b)$$

These results reduce to Eq. (2.6-7) in the case of memoryless characteristics.

## NUMERICAL SOLUTION OF THE DF INTEGRAL

For simplicity, the following development is limited to *odd* nonlinear characteristics which may have memory. The DF can be written as

$$N(A) = \frac{2}{\pi A}\int_0^{\pi} y(A\sin\psi)\sin\psi\, d\psi + j\frac{2}{\pi A}\int_0^{\pi} y(A\sin\psi)\cos\psi\, d\psi$$

$$= \frac{2}{\pi A}\int_{\psi=0}^{\psi=\pi} y(A\sin\psi)\, d(-\cos\psi) + j\frac{2}{\pi A}\int_{\psi=0}^{\psi=\pi} y(A\sin\psi)\, d(\sin\psi) \quad (2.6\text{-}11)$$

These integrals can be approximated by finite sums. In so doing, it is helpful to write separately the integrals over two ranges in $\psi$, from 0 to $\pi/2$ and from

$\pi/2$ to $\pi$. Thus

$$N(A) = \frac{2}{\pi A}\left[\int_{\psi=0}^{\psi=\pi/2} y(A\sin\psi)\, d(-\cos\psi) + \int_{\psi=\pi/2}^{\psi=\pi} y(A\sin\psi)\, d(-\cos\psi)\right]$$
$$+ j\frac{2}{\pi A}\left[\int_{\psi=0}^{\psi=\pi/2} y(A\sin\psi)\, d(\sin\psi) + \int_{\psi=\pi/2}^{\psi=\pi} y(A\sin\psi)\, d(\sin\psi)\right]$$
$$\approx \frac{2}{\pi A}\left[\sum_{i=1}^{n/2} y(A\sin\psi_i)\,\delta(-\cos\psi_i) + \sum_{i=n/2+1}^{n} y(A\sin\psi_i)\,\delta(-\cos\psi_i)\right]$$
$$+ j\frac{2}{\pi A}\left[\sum_{i=1}^{n/2} y(A\sin\psi_i)\,\delta(\sin\psi_i) + \sum_{i=n/2+1}^{n} y(A\sin\psi_i)\,\delta(\sin\psi_i)\right] \tag{2.6-12}$$

It has been assumed that an $n$-term summation is performed, with $n$ even. Taking equal increments of $\delta(-\cos\psi_i)$ in the $n_p$ integration, and equal increments of $\delta(\sin\psi_i)$ in the $n_q$ integration, Eq. (2.6-12) can be rewritten as

$$N(A) \approx \frac{2}{\pi A}\,|\delta(-\cos\psi)|\left[\sum_{i=1}^{n/2} y(A\sin\psi_i) + \sum_{i=n/2+1}^{n} y(A\sin\psi_i)\right]$$
$$+ j\frac{2}{\pi A}\,|\delta(\sin\psi)|\left[\sum_{i=1}^{n/2} y(A\sin\psi_i) - \sum_{i=n/2+1}^{n} y(A\sin\psi_i)\right] \tag{2.6-13}$$

The minus sign in the second set of brackets results from the fact that the sign of the increment $\delta(\sin\psi_i)$ is negative for $\psi$ increasing from $\pi/2$ to $\pi$ (that is, $i$ increasing from $n/2+1$ to $n$).

Both of the uniform increment magnitudes, $|\delta(-\cos\psi)|$ and $|\delta(\sin\psi)|$, can be seen to have the value $2/n$. Calling

$$u_i = \sin\psi_i$$

we can write the compact expression

$$N(A) \approx \frac{2}{\pi A}\frac{2}{n}\sum_{i=1}^{n} y(Au_i) + j\frac{2}{\pi A}\frac{2}{n}\sum_{i=1}^{n} S_i\, y(Au_i) \tag{2.6-14}$$

which is the result sought. The term $S_i$ accounts for the sign change in the $n_q$ integration; viz.,

$$S_i = \begin{cases} +1 & \text{for } 1 \le i \le \dfrac{n}{2} \\ -1 & \text{for } \dfrac{n}{2}+1 \le i \le n \end{cases}$$

Observe that $u_i$ goes from 0 to 1 and back to 0, as $\psi$ varies from 0 to $\pi/2$ to $\pi$. The values of $u_i$ give the points at which $y(Au)$ is evaluated. These

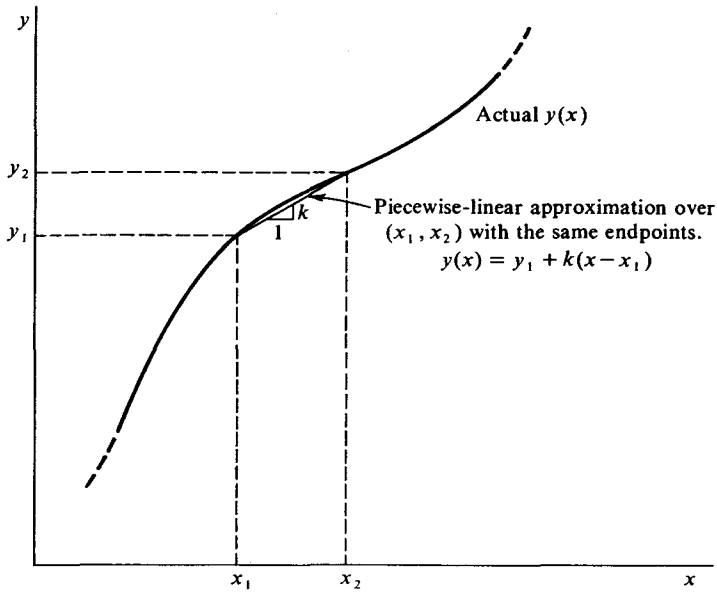


*Figure 2.6-2 Approximation for numerical integration over one segment of the nonlinear characteristic.*

points should be chosen so that the summations of Eq. (2.6-14) are good approximations to the corresponding integrals of Eq. (2.6-11). One reasonable way to choose the $u_i$ is to require that the approximation to each integral be exact for an "average" function, perhaps a function which is linear over each summation interval and has the same endpoints (Fig. 2.6-2). The result of this choice for the $u_i$ is just the well-known trapezoidal integration rule.

Consider the terms relevant to the $n_q$ integration. From Eq. (2.6-11) we have, for a typical summation interval $(u_1,u_2)$,

$$\int_{u_1}^{u_2} y(Au)\,du \approx \int_{u_1}^{u_2} [y_1 + kA(u - u_1)]\,du$$

$$= (u_2 - u_1)(y_1 - kAu_1) + \frac{kA}{2}(u_2^2 - u_1^2)$$

and from Eq. (2.6-14) the corresponding *term* is

$$|\delta u|\, y(Au_i) = (u_2 - u_1)[y_1 + kA(u_i - u_1)]$$

Equating these quantities yields

$$u_i = \frac{u_1 + u_2}{2} \qquad \text{for the } n_q \text{ integration}$$

A parallel development for the $n_p$ integration results in the determination that[1]

$$u_i = \frac{\sin^{-1} u_2 - \sin^{-1} u_1 - u_2\sqrt{1-u_2^2} + u_1\sqrt{1-u_1^2}}{2(\sqrt{1-u_1^2} - \sqrt{1-u_2^2})}$$

for the $n_p$ integration

In each case $u_i$ is the value of $u$, intermediate to $u_1$ and $u_2$, at which $y(Au_i)$ is evaluated. The values of $u_i$ for $n = 10$ and $n = 20$ are given in Table 2.6-1.

**TABLE 2.6-1 VALUES OF $u_i$ FOR DF DETERMINATION BY TRAPEZOIDAL INTEGRATION**

| $n_p$ integration | | $n_q$ integration | |
|---|---|---|---|
| $n = 10$ | $n = 20$ | $n = 10$ | $n = 20$ |
| $u_i = 0.4088$ | $u_i = 0.2936$ | $u_i = 0.10$ | $u_i = 0.05$ |
| 0.7095 | 0.5239 | 0.30 | 0.15 |
| 0.8634 | 0.6600 | 0.50 | 0.25 |
| 0.9520 | 0.7590 | 0.70 | 0.35 |
| 0.9933 | 0.8344 | 0.90 | 0.45 |
| | 0.8924 | | 0.55 |
| | 0.9362 | | 0.65 |
| | 0.9678 | | 0.75 |
| | 0.9882 | | 0.85 |
| | 0.9983 | | 0.95 |

These integration formulas are particularly easy to use with a desk calculator since no multiplication is required to scale the values of $y(Au_i)$, which are read from a graph of $y(x)$ or computed. Using 10 increments per unity interval in $u$ in each summation, one can expect DF computation accuracies of better than 5 percent.

## PLACING BOUNDS ON THE DF

In any DF calculation a convenient independent check is certainly desirable. The general shape of the DF as a function of $A$ can be easily determined by inspection of the nonlinear characteristic in question. Quantitative estimates, we shall see, are also feasible.

Consider an arbitrary nonlinear function $y(x)$ for which we seek DF information, and two associated curves $y_u(x)$ and $y_l(x)$. The latter curves are

[1] This is readily shown with the aid of the identities:

$$\int \frac{u\,du}{\sqrt{1-u^2}} = -\sqrt{1-u^2} \qquad \int \frac{u^2\,du}{\sqrt{1-u^2}} = \tfrac{1}{2}(\sin^{-1} u - u\sqrt{1-u^2})$$

required to bound $y(x)$ from above and below, respectively, but are otherwise arbitrary. Odd single-valued characteristics are assumed for convenience. The following inequality then holds for all $x$ in the range of interest.

$$y_l(x) < y(x) < y_u(x) \qquad \text{for } 0 < x < A_1 \tag{2.6-15}$$

where $A_1$ defines the highest value of $x$ of interest. This implies the integral inequality

$$\int_0^{\pi/2} y_l(A \sin \psi) \sin \psi \, d\psi < \int_0^{\pi/2} y(A \sin \psi) \sin \psi \, d\psi < \int_0^{\pi/2} y_u(A \sin \psi) \sin \psi \, d\psi \tag{2.6-16}$$

which may be rewritten as the DF inequality

$$N_l(A) < N(A) < N_u(A) \tag{2.6-17}$$

where $N_l(A)$ and $N_u(A)$ are the DFs belonging to $y_l(x)$ and $y_u(x)$, respectively. Hence bounds may be placed on $N(A)$ provided only that $N_l(A)$ and $N_u(A)$ are known.

The most convenient functions $y_u(x)$ and $y_l(x)$ are simply straight lines passing through the origin. If the lines have slopes $k_u$ and $k_l$, then we have, simply,

$$k_l < N(A) < k_u \tag{2.6-18}$$

Figure 2.6-3 illustrates the application of this simple bounding process to a typical nonlinear characteristic. Stronger bounds on $N(A)$ can be obtained by choosing better upper and lower nonlinearity bounding functions.

## 2.7 DF INVERSION

Given the DF data $n_p(A)$ and $n_q(A)$, one may be interested in a nonlinearity to which this corresponds. This inverse DF question is of interest in the evaluation of a physical device whose harmonic response has been experimentally obtained, and in the synthesis of a nonlinear compensatory network whose DF has been prescribed. It is intuitively clear that since the DF is an incomplete measure of a nonlinear characteristic, DF inversion is necessarily nonunique. For example, one can readily find nonlinear characteristics with memory which possess DFs identical with other characteristics with no memory (cf. Prob. 2-13). Below, we consider several cases where $n_q(A) = 0$ and the recovered memoryless nonlinearity is odd. The extension to asymmetric nonlinearities is straightforward, although of less interest. For a treatment of the more general case in which $n_q(A) \neq 0$, the reader is referred to Gibson et al. (Ref. 13), where an analytic DF inversion solution is developed.

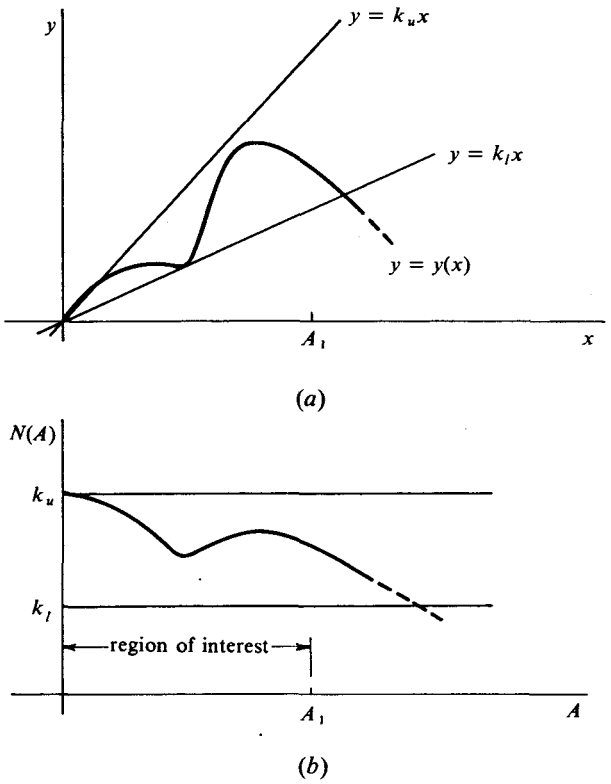


***Figure 2.6-3*** *Bounding of the DF (b) by forming a straight-line envelope for the nonlinear characteristic (a).*

## POLYNOMIAL-BASED DF INVERSION

Assume that a polynomial curve fit to $N(A)$ has been accomplished. The result is

$$N(A) = \sum_{k=0}^{n} a_k A^k \tag{2.7-1}$$

In Sec. 2.3 it was demonstrated that for an odd-polynomial $n$th-order nonlinearity the DF is given by

$$N(A) = \frac{2}{\pi} \sum_{k=1}^{n} c_k A^{k-1} \frac{\Gamma[(k+2)/2]}{\Gamma[(k+3)/2]} \tag{2.7-2}$$

By comparing Eqs. (2.7-1) and (2.7-2) we immediately establish the result

$$c_k = \frac{\pi}{2} \frac{\Gamma[(k+3)/2]}{\Gamma[(k+2)/2]} a_{k-1} \tag{2.7-3}$$

which defines an odd-polynomial nonlinearity.

## PIECEWISE-LINEAR-BASED DF INVERSION

In Sec. 2.3 it was shown that the DF for an odd $n$-segment, piecewise-linear memoryless nonlinearity can be written in the form

$$N(A) = \frac{4M}{\pi A} + \sum_{i=1}^{n-1} (m_i - m_{i+1}) f\left(\frac{\delta_i}{A}\right) + m_n \tag{2.7-4}$$

If $M \neq 0$, assume that it is removed from Eq. (2.7-4) by a curve fit in the vicinity of $A \approx 0$. The nonlinear characteristic to be determined thus has a discontinuity of value $2M$ at the origin. Now let the DF-data abscissa be divided into equal subdivisions of width $\delta$. By computing $N(A)$ for $A = \delta/2,\ 3\delta/2,\ 5\delta/2$, etc., the following set of equations results from the repeated application of Eq. (2.7-4):

$$\begin{aligned} N\left(\frac{\delta}{2}\right) &= m_1 \\ N\left(\frac{3\delta}{2}\right) &= (m_1 - m_2) f(\tfrac{2}{3}) + m_2 \\ N\left(\frac{5\delta}{2}\right) &= (m_1 - m_2) f(\tfrac{2}{5}) + (m_2 - m_3) f(\tfrac{4}{5}) + m_3 \\ &\cdots\cdots\cdots\cdots\cdots\cdots\cdots\cdots \end{aligned} \tag{2.7-5}$$

This set is easily solved by applying the solution for $m_1$ from the first equation to the second, then using the resulting solution for $m_2$ in the third, and so forth. For sufficiently small $\delta$, the nonlinearity so determined will closely represent the required nonlinearity. If the nonlinearity for which the DF was determined actually was piecewise-linear, and if $\delta$ happens to be chosen at a value which is some integral fraction of each breakpoint, $\delta_i$, of the actual nonlinearity, the piecewise-linear function determined by means of Eq. (2.7-5) will be precisely the actual nonlinearity.

## APPROXIMATE DF INVERSION

By repeated application of the approximate DF formula [Eq. (2.6-7)] it is possible to secure an approximate DF inversion.

$$\begin{aligned} N(A) &\approx \frac{2}{3A}\left[y(A) + y\left(\frac{A}{2}\right)\right] \\ N(2A) &\approx \frac{1}{3A}\left[y(2A) + y(A)\right] \\ N(4A) &\approx \frac{1}{6A}\left[y(4A) + y(2A)\right] \\ &\cdots\cdots\cdots\cdots\cdots \end{aligned} \tag{2.7-6}$$

Starting with the first equation above, and inserting in it the values for $y(A)$, $y(2A)$, $y(4A)$, etc., appearing in subsequent equations, we easily generate the result

$$\begin{aligned} y\left(\frac{A}{2}\right) &\approx \frac{3A}{2} N(A) - y(A) \\ &\approx \frac{3A}{2} N(A) - 3AN(2A) + y(2A) \\ &\approx \frac{3A}{2} N(A) - 3AN(2A) + 6AN(4A) - y(4A) \\ &\quad \cdots\cdots\cdots\cdots\cdots\cdots\cdots\cdots \end{aligned} \tag{2.7-7}$$

which is expressible as

$$y(A) \approx 3A \sum_{i=0}^{\infty} (-2)^i N(2^{i+1}A) \tag{2.7-8}$$

Had we instead employed the relationships

$$\begin{aligned} N(A) &\approx \frac{2}{3A}\left[y(A) + y\left(\frac{A}{2}\right)\right] \\ N\left(\frac{A}{2}\right) &\approx \frac{4}{3A}\left[y\left(\frac{A}{2}\right) + y\left(\frac{A}{4}\right)\right] \\ N\left(\frac{A}{4}\right) &\approx \frac{8}{3A}\left[y\left(\frac{A}{4}\right) + y\left(\frac{A}{8}\right)\right] \\ &\quad \cdots\cdots\cdots\cdots\cdots\cdots \end{aligned} \tag{2.7-9}$$

and proceeded as in Eq. (2.7-7), the corresponding result would be

$$y(A) \approx \frac{3A}{2} \sum_{i=0}^{\infty} (-\tfrac{1}{2})^i N\left(\frac{A}{2^i}\right) \tag{2.7-10}$$

Equations (2.7-8) and (2.7-10) are the approximate DF inversion formulas sought. The former is applied to a given set of DF data when the values of $N(A)$ decrease with increasing values of $A$, thus leading to a rapidly converging series for $y(A)$. In the opposite case, Eq. (2.7-10) is employed. In either case the resulting function is $y(x)$.

**Example 2.7-1** Given the DF data $N(A) = 4D/\pi A$, employ Eq. (2.7-10) to find a corresponding $y(x)$.

In this case one must proceed with some care to ensure that the series expansion for $y(A)$ converges. Consider the replacement of Eq. (2.7-10) by

$$y(A) \approx \frac{3A}{2} \lim_{\epsilon \to 1} \sum_{i=0}^{\infty} \left(-\frac{\epsilon}{2}\right)^i N\left(\frac{A}{2^i}\right) \tag{2.7-11}$$

Inserting the given DF data, we now get

$$y(A) \approx \frac{3A}{2} \lim_{\epsilon \to 1} \sum_{i=0}^{\infty} \left(-\frac{\epsilon}{2}\right)^i \frac{4D}{\pi A} (2^i)$$

$$= \frac{6D}{\pi} \lim_{\epsilon \to 1} \sum_{i=0}^{\infty} (-\epsilon)^i$$

$$= \frac{6D}{\pi} \lim_{\epsilon \to 1} \frac{1}{1+\epsilon}$$

$$= \frac{3D}{\pi}$$

The reason for the particular form chosen for Eq. (2.7-11) is at once evident, since without it (and the understanding that $\epsilon$ approaches 1 from below), the resulting infinite series would have been the alternating series $1 - 1 + 1 - 1 + 1 - \cdots$, etc.

Interpreting the result as an odd single-valued nonlinearity, it follows that the characteristic is described by

$$y(x) = \begin{cases} \dfrac{3D}{\pi} & \text{for } x \geq 0 \\ -\dfrac{3D}{\pi} & \text{for } x < 0 \end{cases}$$

which the reader from the outset knew to be an ideal-relay characteristic. The inversion is thus in error by 4.5 percent. Aside from cases where $N(A)$ is inversely proportional to $A$ (such as in this example), no special precaution need be taken, and Eqs. (2.7-8) and (2.7-10) can be freely employed.

Up to this point we have developed the facility to calculate DFs for a very wide class of nonlinearities. In the following chapter we turn our attention to the use of these DFs in the study of nonlinear feedback systems.

## REFERENCES


1. Andronow, A. A., and C. E. Chaikin: "Theory of Oscillations," Princeton University Press, Princeton, N.J., 1949.
2. Bhattacharyya, B. P.: Describing-function Expressions for Sine-type Functional Nonlinearity in Feedback Control Systems, *J. IEE*, vol. B-108, no. 41 (September, 1961), pp. 529–534.
3. Casserly, G., and J. G. Truxal: Measurement and Stabilization of Nonlinear Feedback Systems, *IRE Conv. Record*, pt. 4 (1956), pp. 52–60.
4. Choudhoury, A. K., M. S. Basu, and A. K. Mahalanabis: A Transfer Function Analyzer for Linear and Nonlinear Components, *Electron. Eng.*, London, vol. 33 (June, 1961), pp. 382–385.
5. Clegg, J. C.: A Nonlinear Integrator for Servomechanisms, *Trans. AIEE*, pt. II, *Appl. Ind.*, vol. 77 (March, 1958), pp. 41–42.

6. Cunningham, W. J.: "Introduction to Nonlinear Analysis," McGraw-Hill Book Company, New York, 1958.
7. Deekshatulu, B. L.: A Graphical Method of Evaluating the Describing Function, *Trans. AIEE*, pt. II, *Appl. Ind.*, vol. 81 (July, 1962), pp. 101–106.
8. Dotort, I. K.: Harmonic Analysis by Direct Area Measurements, *Trans. AIEE*, pt. II, *Appl. Ind.*, vol. 75 (March, 1956), pp. 16–19.
9. Douce, J. L.: A Note on the Evaluation and Response of a Non-linear Element to Sinusoidal and Random Signals, *J. IEE* (London), vol. C-105 (October, 1957), p. 88.
10. Dutilh, J.: Théorie des servoméchanisms à relais, *Onde Élec.*, vol. 30 (1950), pp. 438–445.
11. Freeman, E. A.: The Effect of Speed-dependent Friction and Backlash on the Stability of Automatic Control Systems, *Trans. AIEE*, pt. II, *Appl. Ind.*, vol. 78 (January, 1959), pp. 680–691.
12. Gibson, J. E., and K. S. Prasanna-Kumar: A New RMS Describing Function for Single-valued Nonlinearities, *Proc. IRE*, vol. 49 (August, 1961), p. 1321.
13. Gibson, J. E., E. G. di Tada, J. C. Hill, and E. S. Ibrahim: Describing Function Inversion: Theory and Computational Techniques, *Purdue Univ., Control Inform. Systems Lab.* TR-EE62-1D, Lafayette, Ind., December, 1962.
14. Gille, J. C., M. J. Pelegrin, and P. Decaulne: "Feedback Control Systems," McGraw-Hill Book Company, New York, 1959.
15. Goldfarb, L. C.: On Some Nonlinear Phenomena in Regulatory System, *Avtomatika i Telemekhanika*, vol. 8, no. 5 (1947), pp. 349–383 (in Russian). Translation: U. Oldenburger (ed.), "Frequency Response," The Macmillan Company, New York, 1956.
16. Graham, D., and D. McRuer: "Analysis of Nonlinear Control Systems," John Wiley & Sons, Inc., New York, 1961.
17. Grief, H. D.: Describing Function of Servomechanism Analysis Applied to Most Commonly Encountered Nonlinearities, *Trans. AIEE*, pt. II, *Appl. Ind.*, vol. 72 (September, 1953), pp. 243–248.
18. Grobner, W., and N. Hofreiter: "Integraltafel," 3d ed., Springer-Verlag OHG, Berlin, 1961.
19. Gronner, A. D.: The Describing Function of Backlash Followed by a Dead Zone, *Trans. AIEE*, pt. II, *Appl. Ind.*, vol. 77 (November, 1958), pp. 403–409.
20. Haas, V. B., Jr.: Coulomb Friction in Feedback Control Systems, *Trans. AIEE*, pt. II, *Appl. Ind.*, vol. 72 (May, 1953), pp. 119–126.
21. Hamos, L. v.: Beitrag zur Frequenzanalyse von nichtlinearen Systemen, "Regelungstechnik: Moderne Theorien und ihre Verwendbarkeit," R. Oldenbourg KG, Munich, 1957, pp. 211–215 (in German).
22. Hartel, W.: Abschätzung der Oberwellen bei gleichstromvormagnetisierten Drosseln, *Arch. Elektrotech.*, vol. 36 (1942), p. 556.
23. Jahnke, E., and F. Emde: "Tables of Functions," 4th ed., Dover Publications, Inc., 1945.
24. Jopling, A. D., and R. A. Johnson: The Elliptic Describing Function, *Proc. Joint Autom. Control Conf.*, Stanford, Calif., June, 1964, pp. 175–184.
25. Kavanagh, R. J.: An Approximation to the Harmonic Response of Saturating Devices, *J. IEE* (London), vol. C-107, no. 11 (January, 1960), pp. 127–133.
26. Klotter, K.: An Extension of the Conventional Concept of the Describing Function, *Proc. Symp. Nonlinear Circuit Analysis*, Polytechnic Institute of Brooklyn, New York, April, 1956, pp. 151–162.
27. Kochenburger, R. J.: Analysis and Synthesis of Contactor Servomechanisms, Sc.D. thesis, Massachusetts Institute of Technology, Department of Electrical Engineering, Cambridge, Mass., 1949.

28. Kochenburger, R. J.: Limiting in Feedback Control Systems, *Trans. AIEE*, pt. II, *Appl. Ind.*, vol. 72 (July, 1953), pp. 180–194.
29. Krylov, N., and N. Bogoliubov: "Introduction to Nonlinear Mechanics," Princeton University Press, Princeton, N.J., Annals of Mathematics Studies, vol. 11, 1947.
30. Ku, Y. H., and C. F. Chen: A New Approach to the Evaluation and Interpretation of Describing Functions, *AIEE Paper* CP61-1084, September, 1961.
31. Lakshmi-Bai, C.: Transformation Method for the Study of Non-linear Components, *Trans. AIEE*, pt. II, *Appl. Ind.*, vol. 79 (September, 1960), pp. 249–254.
32. Lauber, R.: A New Method to Derive the Describing Function of Certain Nonlinear Transfer Systems, *Proc. IFAC*, Basel, Switzerland, August, 1963, pp. 188/1–188/5.
33. Levinson, E.: Non-linear Feedback Control Systems, pt. 3, *Electro-Technology*, vol. 72 (September, 1962), pp. 136–146.
34. Levinson, E.: Gain-Phase Relations of Nonlinear Circuits, *IRE Conv. Record*, pt. IV, 1958, pp. 141–159.
35. Lory, H. L., D. C. Lai, and W. H. Huggins: On the Use of Growing Harmonic Exponentials to Identify Static Nonlinear Operators, *IRE Trans. Autom. Control*, vol. AC-4, no. 2 (November, 1959), pp. 91–99.
36. Magnus, K.: "Über ein Verfahren zur Untersuchung nicht-linearer Schwingungs- und Regelungs-Systeme," VDI-Verlag GmbH, Düsseldorf, Germany, 1955. Translated into English by the Langley Research Center, NASA, Hampton, Va., October, 1958.
37. Makow, D. M.: Harmonic Analysis and Describing Function of Nonlinear Systems, *IRE Intern. Conv. Record*, pt. 4, 1961, pp. 69–76.
38. McBride, L. E., Jr.: Approximate Describing Function for Double-valued Nonlinearities, *Electronics Letters*, London, vol. 1, no. 3 (May, 1965).
39. Mishkin, E., and L. Braun, Jr.: "Adaptive Control Systems," McGraw-Hill Book Company, New York, 1961.
40. Neilsen, K. L.: "Methods in Numerical Analysis," The Macmillan Company, New York, 1956.
41. Oppelt, W.: Locus Curve Method for Regulators with Friction, *Z. Deut. Ingr.*, Berlin, vol. 90 (1948), pp. 179–183. Translated in *Report* 1691, National Bureau of Standards, Washington, 1952.
42. Poincaré, H.: "Les méthodes nouvelles de la mécanique celéste," vol. 1, Gauthier-Villars, Paris, 1892; reprinted by Dover Publications, Inc., New York, 1957.
43. Rankine, R. R., Jr., and J. J. D'Azzo: A Corrected-conventional Describing Function for Intermediate-order Nonlinear Control Systems, *Proc. Northeast Electronics Res. Eng. Meeting*, November, 1964, pp. 38–39.
44. Satyendra, K. N.: Describing Functions Representing the Effect of Inertia, Backlash and Coulomb Friction on the Stability of an Automatic Control System, I, *Trans. AIEE*, pt. II, *Appl. Ind.*, vol. 75 (September, 1956), pp. 243–249.
45. Semmelhack, H. P., and P. M. DeRusso: A Nonsinusoidal Describing Function for Stiction and Coulomb Friction, *IEEE Paper* CP63-921.
46. Silberberg, M. Y.: A Note on the Describing Function of an Element with Coulomb, Static, and Viscous Friction, *Trans. AIEE*, pt. II, *Appl. Ind.*, vol. 76 (January, 1957), pp. 423–425.
47. Sridhar, R.: A General Method for Deriving the Describing Functions for a Certain Class of Nonlinearities, *IRE Trans. Autom. Control*, vol. AC-5, no. 2 (June, 1960), pp. 135–141.
48. Stein, W. A., and G. J. Thaler: Obtaining the Frequency Response Characteristics of a Nonlinear Servomechanism from an Amplitude- and Frequency-sensitive Describing Function, *Trans. AIEE*, pt. II, *Appl. Ind.*, vol. 77 (May, 1958), pp. 91–96.
49. Stoker, J. J.: "Non-linear Vibrations in Mechanical and Electrical Systems," Interscience Publishers, Inc., New York, 1950.

50. Stout, T. M.: Block Diagram Transformations for Systems with One Nonlinear Element, *Trans. AIEE*, pt. II, *Appl. Ind.*, vol. 75 (July, 1956), pp. 130–141.
51. Tsypkin, Ya. Z.: Discussion of a paper by J. C. West, in "Regelungstechnik: Moderne Theorien und ihre Verwendbarkeit," R. Oldenbourg KG, Munich, 1957, pp. 163–164 (in German).
52. Tustin, A.: The Effects of Backlash and of Speed Dependent Friction on the Stability of Closed-cycle Control Systems, *J. IEE* (London), vol. 94, pt. II (May, 1947), pp. 143–151.
53. von Wyss, M. R.: The Describing Function for Saturated Amplification in Series with Saturated Integration, *SAAB Tech. Note* 46, Saab Aircraft Company, Linköping, Sweden, 1960.
54. Watson, G. N.: "A Treatise on the Theory of Bessel Functions," Cambridge University Press, New York, 1922, chap. 10.
55. West, J. C.: The Describing Function Technique Applied to Non-linear Systems, Part I, *Process Control and Automation*, vol. 7 (September, 1960), pp. 421–426.
56. Zaborsky, J., and H. J. Harrington: Describing Function for Hydraulic Valves, *Trans. AIEE*, pt. I, vol. 76 (1957), pp. 183–198.
57. Zakharov, K. V., and V. K. Svyatodukh: An Instrument for Determining the Frequency Characteristics of Nonlinear Systems, *Automation and Remote Control*, vol. 21 (June, 1960), pp. 1630–1637.

## PROBLEMS

2-1. Show by use of the perturbation method that the first-order corrected fundamental component of the solution to the problem of a mass on a nonlinear spring

$$\ddot{x} + \omega_0^2 x + \mu x^3 = 0$$

subject to the initial conditions

$$x(0) = A_0 \qquad \dot{x}(0) = 0$$

is given by

$$x = A_0\left(1 - \frac{\mu A_0^2}{32\omega^2}\right)\cos \omega t$$

$$\omega^2 = \omega_0^2 + \frac{3\mu A_0^2}{4}$$

2-2. Show by use of the method of slowly varying amplitude and phase that the solution to Prob. 2-1 is

$$x = A_0 \cos \omega t$$

$$\omega = \omega_0 + \frac{3\mu A_0^2}{8\omega_0}$$

2-3. By use of the method of Krylov and Bogoliubov, show that the approximate transient solution to Van der Pol's equation

$$\ddot{x} - \epsilon(1 - x^2)\dot{x} + x = 0$$

is given by

$$x = \frac{A_0 e^{(\epsilon/2)t}}{\sqrt{1 + (A_0^2/4)(e^{\epsilon t} - 1)}} \sin(t + \theta_0)$$

where $A_0$ and $\theta_0$ define the initial state of the system. Discuss the relationship between the system steady state and its initial conditions.

2-4. Derive the DF for an odd quantizer nonlinearity with arbitrarily spaced breakpoints $\delta_i$ and arbitrary output levels $D_i$.

2-5. Derive the overall DF for the following chain of elements: ideal relay–integrator–ideal relay. The integrator gain is $K$, and the relay drive levels are $\pm D$.

2-6. By noting that (rotary) coulomb friction is a torque-velocity phenomenon, show that the DF relating input rotation *angle* to output torque is

$$N(A,\omega) = \frac{4T}{\pi A} e^{(j\pi/2)}$$

where $T$ is the coulomb-friction magnitude, and $A$ is the input-angle amplitude.

Using this result, find the DF (angle input–angle output) for spring-coupled coulomb friction (massless case), and compare it with that for spring-coupled viscous friction.

What is the DF for inertia with coulomb friction (torque input–angle output)?

2-7. A useful technique for obtaining DFs for functionally characterized nonlinearities is to generate the power series of these functions in order to apply DF results already developed for polynomials. Using this technique, find DFs for the following nonlinear characteristics, and discuss the range of validity of each:

(*a*) $y = \tanh^{-1} x$

(*b*) $y = 1 - e^{-|x|}$

(*c*) $y = \dfrac{\sin x}{|x|}$

(*d*) $y = x \cos x$

2-8. Obtain the DF and third-harmonic amplitude ratio for the nonlinear characteristic of Fig. 2-1, such as might correspond to an optical-tracker error signal as a function of tracker misalignment in a satellite attitude control system. (*Hint:* Approximations may prove expedient.)

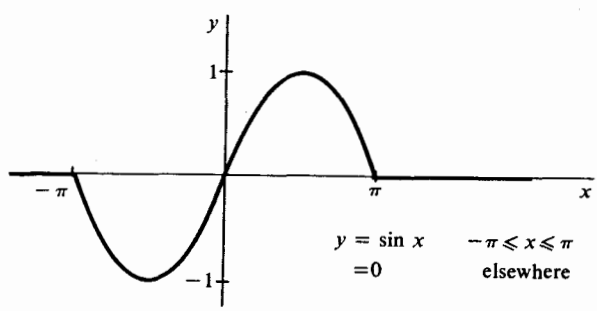


***Figure 2-1*** *Optical-tracker error characteristic.*

2-9. In determining the DF for a *dynamic* element of the form

$$y = f(\dot{x})$$

is it legitimate to simply observe the block-diagram equivalence of Fig. 2-2, and hence conclude the relationship

$$N_{\dot{x}}(A,\omega) = sN_x(A)$$

where $N_x(A)$ is the DF for the *static* nonlinearity $f(x)$?

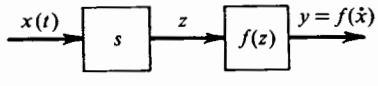


***Figure 2-2*** *Series dynamic nonlinearity.*

2-10. Find the DF for the parallel-connected dynamic nonlinearity system of Fig. 2-3. How would you recommend testing this two-port system to experimentally determine parameters $\delta_1$, $D_1$, $\delta_2$, and $D_2$, knowing a priori the form of the nonlinearity?

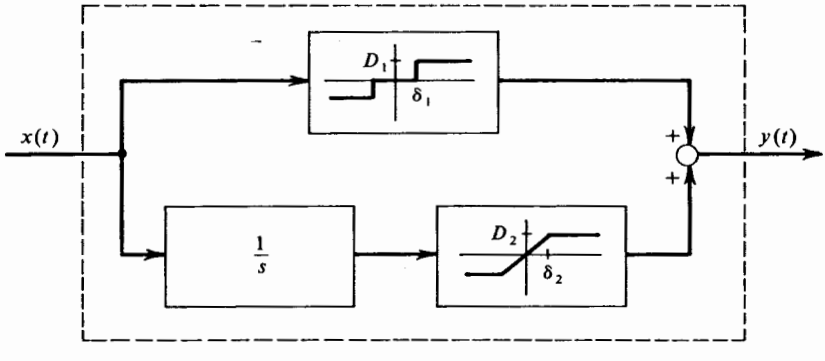


***Figure 2-3*** *Parallel dynamic nonlinearity.*

2-11. The nonlinear element described by

$$\ddot{y} + \dot{y}^3 = x$$

is imbedded in a larger system to be analyzed by DF methods. Find the DF for this nonlinear element.

2-12. Find and graph the DF for the nonlinear element of Fig. 2-4. By also plotting DFs for the two limiters (drawn dotted), show that the original DF is bounded above and below.

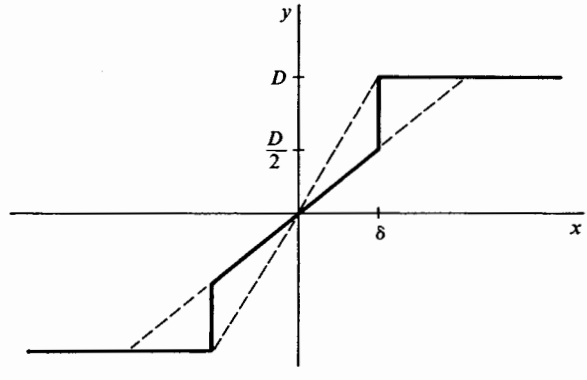


*Figure 2-4 Nonlinearity with linear zone and abrupt limiting.*

2-13. (*a*) Derive the DF for the nonlinear characteristic with memory of Fig. 2-5, and hence demonstrate that it is non-phase-shifting.
(*b*) Synthesize the same DF by parallel addition of several memoryless nonlinearities, and hence demonstrate that DF inversion is indeed not unique.

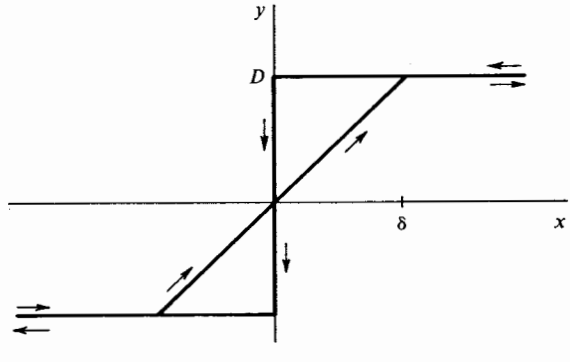


*Figure 2-5 Nonlinear characteristic with memory.*

2-14. In a certain torque feedback servo loop, the torquer input current is derived from a current supply with a piecewise-linear limiter characteristic (input breakpoints $\pm\delta$ and output saturation levels $\pm D$). The torque generator has an odd square-law characteristic from input current to output torque. Show that the DF from current-supply input command to torque-generator output torque is

$$N(A) = \frac{8}{3\pi}\left(\frac{D}{\delta}\right)^2 A\left\{1 - \left[1 - \left(\frac{\delta}{A}\right)^2\right]^{\frac{3}{2}}\right\}$$

2-15. Show that the exact DF for the nonlinear chain illustrated in Fig. 2-6 is given by

$$N(A,\omega) = \begin{cases} \dfrac{4D_1KD_2}{\pi\delta\omega A} \sin\left(\dfrac{\delta\omega}{D_1K}\right) e^{-j\pi/2} & \text{for } \dfrac{\delta\omega}{D_1K} \leq \dfrac{\pi}{2} \\ \dfrac{4D_1KD_2}{\pi\delta\omega A} e^{-j\pi/2} & \text{for } \dfrac{\delta\omega}{D_1K} > \dfrac{\pi}{2} \end{cases}$$

and compare this with the result obtained by multiplying the DFs of the individual elements of the chain. Under what conditions does DF multiplication yield an acceptable solution?

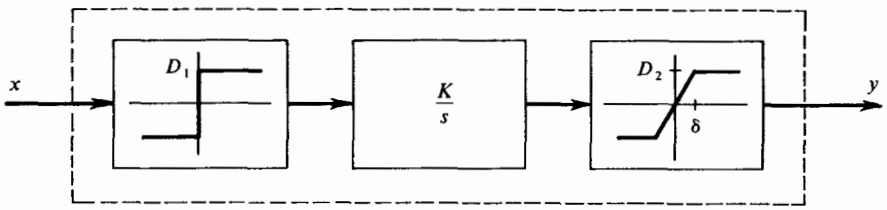


***Figure 2-6*** *Dynamic multiple-nonlinearity chain.*

2-16. One form of slowly saturating nonlinear characteristic is governed by Froelich's equation

$$y = \frac{x}{1 + c\,|x|}$$

Plot the appropriately normalized DF for this characteristic, and compare it with the DF for a limiter with the same slope at the origin and the same peak output level. Discuss the shape of characteristic and DF for the nonlinearity

$$y = \left(\frac{x}{1 + c\,|x|}\right)^n$$

for values $n < 1$ and $n > 1$.

2-17. The Chebyshev polynomial of order $k$ is given by

$$T_k(x) = \cos(k \cos^{-1} x)$$

(*a*) Show that the $k$th-harmonic amplitude in the output of a sinusoidally forced static single-valued nonlinearity $y(x)$ can be written in the form ($k \geq 1$)

$$A_k = \frac{2}{\pi} \int_{-A}^{A} y(x) T_k\left(\frac{x}{A}\right) \frac{dx}{\sqrt{A^2 - x^2}}$$

where $A$ is the input amplitude.

(*b*) Next, develop a method[1] for recovering the nonlinear characteristic from its

[1] Described by D. P. Atherton: Determination of Nonlinearity from the Harmonic Response, *Electronics Letters*, London, vol. 2, no. 4 (April, 1966), p. 152.

harmonic response by expanding the nonlinearity in the form

$$y(x) = \sum_{l=0}^{\infty} \alpha_l T_l\left(\frac{x}{A}\right)$$

and using the orthogonality relationship

$$\frac{2}{\pi}\int_{-A}^{A} T_l\left(\frac{x}{A}\right) T_k\left(\frac{x}{a}\right) \frac{dx}{\sqrt{A^2 - x^2}} = \begin{cases} 1 & \text{for } k = l \\ 0 & \text{for } k \neq l \end{cases}$$

2-18. Prove the relationship

$$\text{Im } [N(A)] = -\frac{S}{\pi A^2}$$

where $S$ is the area enclosed by $y(x)$ as $x$ varies from zero to $A$ to $-A$ and back to zero, and thereby establish from this point of view that memoryless nonlinearities possess only real DFs. (*Hint:* A contour integral may be helpful.)

2-19. Show that the rms DF and corrected conventional DF for a relay with dead-zone nonlinearity are given by ($A > \delta$)

$$N_{\text{rms}}(A) = \frac{D}{A}\sqrt{\frac{2}{\pi}\left(\pi - 2\sin^{-1}\frac{\delta}{A}\right)}$$

$$N_{\text{ccDF}}(A) = \frac{4D}{\pi A}\sqrt{1 - \left(\frac{\delta}{A}\right)^2}\sqrt{1 + \frac{1}{9}\left[1 - \left(\frac{2\delta}{A}\right)^2\right]^2}$$

2-20. Show that the DF for a flip-flop with first-order dynamic response is given by (see Fig. 2-7):

$$N(A,\omega) = \frac{4D}{\pi A}\frac{1}{1 + j\omega\tau}$$

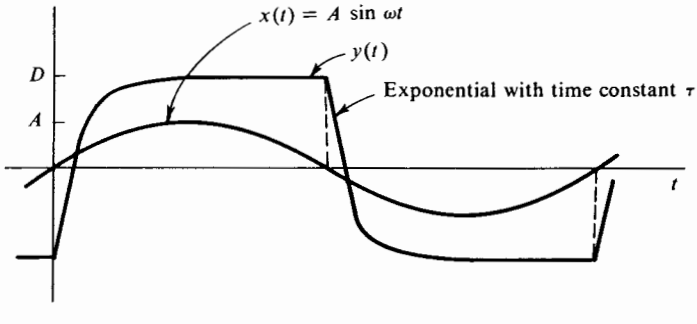


*Figure 2-7 Flip-flop response to input sinusoid.*